JOURNAL OF GEOPHYSICAL RESEARCH, VOL. 112, F03S10, doi:10.1029/2006JF000566, 2007

Formation of fluvial hanging valleys: Theory and simulation

Benjamin T. Crosby,[1,2] Kelin X. Whipple,[1,3] Nicole M. Gasparini,[3,4] and Cameron W. Wobus[1,5]

Received 7 May 2006; revised 7 February 2007; accepted 30 March 2007; published 9 August 2007.

[1] Although only recently recognized, hanging tributary valleys in unglaciated, tectonically active landscapes are surprisingly common. Stream power–based river incision models do not provide a viable mechanism for the formation of fluvial hanging valleys. Thus these disequilibrium landforms present an opportunity to advance our understanding of river incision processes. In this work, we demonstrate that thresholds apparent in sediment flux–dependent bedrock incision rules provide mechanisms for the formation of hanging valleys in response to transient pulses of river incision. We simplify recently published river incision models in order to derive analytical solutions for the conditions required for hanging valley formation and use these results to guide numerical landscape evolution simulations. Analytical and numerical results demonstrate that during the response to base level fall, sediment flux–dependent incision rules may create either temporary or permanent hanging valleys. These hanging valleys form as a consequence of (1) rapid main stem incision oversteepening tributary junctions beyond some threshold slope or (2) low tributary sediment flux response during the pulse of main stem incision, thus limiting the tributary's capacity to keep pace with main stem incision. The distribution of permanent and temporary hanging valleys results from four competing factors: the magnitude of base level fall, the upstream attenuation of the incision signal, the lag time of the sediment flux response, and the nonsystematic variation in tributary drainage areas within the stream network. The development of hanging valleys in landscapes governed by sediment flux–dependent incision rules limits the transmission of base level fall signals through the channel network, ultimately increasing basin response time.

Citation: Crosby, B. T., K. X. Whipple, N. M. Gasparini, and C. W. Wobus (2007), Formation of fluvial hanging valleys: Theory and simulation, *J. Geophys. Res.*, *112*, F03S10, doi:10.1029/2006JF000566.

1. Motivation

[2] When there is a change in the tectonic or climatic forcing on a landscape, hillslopes and channels adjust their form until reestablishing equilibrium with the new boundary conditions. The spatial distribution and response time of this transient adjustment can exert a fundamental influence on the growth and development of mountain ranges, the timing and delivery of sediment to depositional basins and other fundamental processes in tectonically active landscapes. As this signal of adjustment propagates through fluvial systems, it can often be distinguished as an oversteepened reach. This channel reach is referred to as a knickpoint and differentiates the relict, unadjusted portion of the landscape upstream from the incised, adjusting reaches downstream (Figure 1). The origin and evolution of knickpoints has captured the interest of scientists for over a century [*Gilbert*, 1896; *Waldbauer*, 1923; *Penck*, 1924; *Davis*, 1932; *von Engeln*, 1940]. Though much of the recent work examining knickpoints focuses on the transmission of incision signals along main stem channels [*Hayakawa and Matsukura*, 2003; *Haviv et al.*, 2006; *Frankel et al.*, 2007], others have examined the basin-wide distribution of knickpoints [*Weissel and Seidl*, 1998; *Bishop et al.*, 2005; *Bigi et al.*, 2006; *Crosby and Whipple*, 2006; *Berlin and Anderson*, 2007]. Some of these studies recognize that in incising, nonglacial, tectonically active landscapes, knickpoints are commonly located at the junction between tributaries and the incised trunk stream [*Snyder et al.*, 1999; *Crosby and Whipple*, 2006; *Wobus et al.*, 2006]. These knickpoints keep the tributary elevated or 'hung' above the trunk stream. In the present study, we explore potential mechanisms for the formation of these hanging valleys.

[1]Department of Earth, Atmospheric and Planetary Sciences, Massachusetts Institute of Technology, Cambridge, Massachusetts, USA.
[2]Now at Department of Geosciences, Idaho State University, Pocatello, Idaho, USA.
[3]Now at School of Earth and Space Exploration, Arizona State University, Tempe, Arizona, USA.
[4]Department of Geology and Geophysics, Yale University, New Haven, Connecticut, USA.
[5]Now at Cooperative Institute for Research in Environmental Sciences, University of Colorado, Boulder, Colorado, USA.

0148-0227/07/2006JF000566$09.00

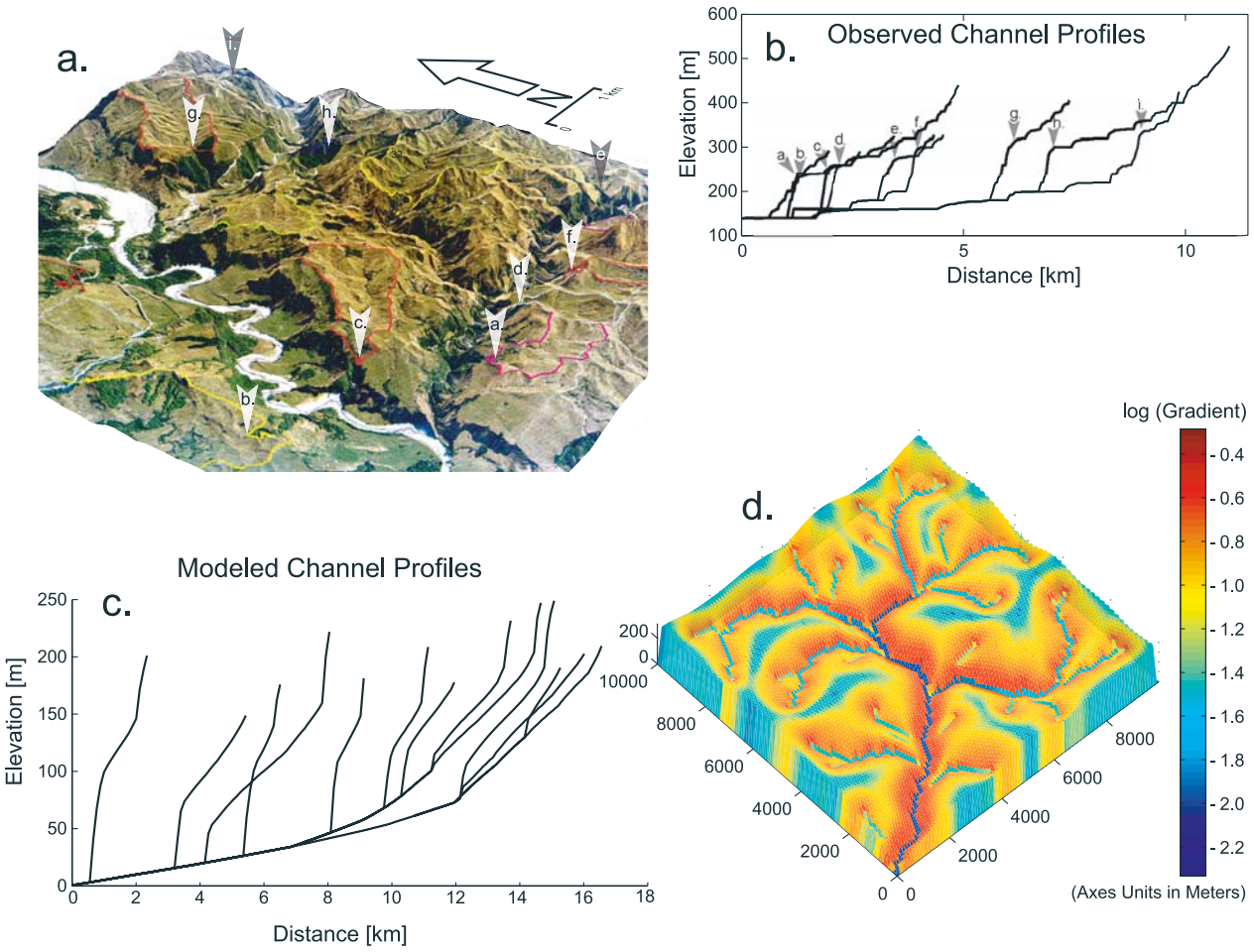

Figure 1. Landscapes responding to a discrete period of incision often possess hanging tributaries or subcatchments isolated above the main stem by a large step in channel elevation. In (a) this topographic rendering of a portion from the Waipaoa River on the North Island of New Zealand, (b) channels draining the outlined tributary basins are elevated above and segregated from the trunk streams by steep knickpoints. In order to understand how these features develop during a transient pulse of incision, we utilize analytical and numerical methods to model (c) the response of channel profiles and (d) drainage basins to discrete base level fall events. Figures 1a and 1b are modified from *Crosby and Whipple* [2006].

[3] The Waipaoa River on the North Island of New Zealand has provided an excellent location to study knickpoint distribution within fluvial basins because the age of disturbance is well established [*Berryman et al.*, 2000; *Eden et al.*, 2001] and there are an abundance of transient landforms such as terraces, incised inner gorges and knickpoints [*Crosby and Whipple*, 2006]. Even in this ideal transient landscape we found it difficult to definitively discern between two proposed mechanisms for the formation of hanging valleys [*Crosby and Whipple*, 2006]. The first proposed mechanism hypothesized that discrete knickpoints migrating up the trunk streams established hanging valleys as the discrete main stem knickpoint passed tributary junctions. The second mechanism proposed that the main stem incised gradually, never containing a distinct knickpoint, but this progressive incision was fast enough to outpace tributary adjustment. The presence and persistence of knickpoints at tributary junctions limits the upstream communication of subsequent signals of base level change into the upper portions of the channel network, thus extending basin response time following disturbance.

[4] The most broadly utilized formulation for fluvial bedrock incision, the detachment-limited stream power model [*Howard and Kerby*, 1983; *Howard*, 1994; *Whipple and Tucker*, 1999] (henceforth simply termed the stream power model), does not predict the formation of hanging tributaries [e.g., *Niemann et al.*, 2001]. This discrepancy between field observation and model behavior suggests a clear inadequacy in standard stream power river incision models. Recently developed sediment flux–dependent bedrock incision relations allow sediment to behave either as a tool for incising the bed or as armor, inhibiting erosion [*Sklar and Dietrich*, 1998; *Whipple and Tucker*, 2002; *Parker*, 2004; *Sklar and Dietrich*, 2004; *Gasparini et al.*, 2006]. We find that these new relations provide mechanisms for explaining the formation and persistence of hanging tributaries at threshold drainage areas [*Crosby and Whipple*, 2006; *Wobus et al.*, 2006; *Gasparini et al.*, 2007]. Indeed, the prevalence of hanging tributaries in

Table 1. Parameters Used During Model Runs

Parameter	Value
Basin dimensions, m	10000×10000
Basin area, m^2	1.0×10^8
Node spacing, m	100
Background rate of base level fall, U, m/yr	1.00×10^{-3}
K_D,[a,b,c,d] m^2/yr	5, 5, 5, 4
Instantaneous base level fall,[e] m	50
Progressive base level fall,[f] m	50
m_t	1.5
n_t	1
K_t, m^{3-2mt}/yr	2.00×10^{-5}
K_{SP}, $m^{-(2m+1)}$	4.00×10^{-5}
K_{SA}, $m^{-0.5}$	5.00×10^{-2}
K_{GA}, m^{-1}	7.00×10^{-3}
m[b,c,d]	0.5, −0.25, 0
n[b,c,d]	1, −0.5, 0
k_w, m^{1-3b}/yr^b	1
b	0.5
k_q, m^{3-2c}/yr	1
c	1
β	0.5

[a]Transport-limited model run.
[b]Detachment-limited stream power model run.
[c]Saltation-abrasion model run.
[d]Generalized abrasion model run.
[e]Discrete elevation change basin outlet.
[f]Increase rate of base level fall 10× and run model until 50 m new of material is exhumed/uplifted.

tool-starved environments may provide the strongest existing field evidence supporting sediment flux–dependent incision rules. Important tasks undertaken here include (1) the quantitative assessment of the conditions under which sediment flux–dependent incision models predict hanging valley formation, and (2) careful determination of what characteristics of these incision models are required by our field observations.

2. Approach and Scope

[5] In this work, we utilize analytical and numerical models to explore whether thresholds in existing relations for stream incision by sediment abrasion provide a plausible mechanism for the formation of hanging valleys. The theoretically demonstrated consequences of these thresholds are then considered relative to existing field studies of the distribution of hanging valleys [*Weissel and Seidl*, 1998; *Bishop et al.*, 2005; *Crosby and Whipple*, 2006; *Wobus et al.*, 2006]. Although plausible alternative explanations for the formation of hanging tributaries exist, thresholds in sediment flux–dependent erosion relations provide an excellent opportunity to compare theoretical predictions against field data.

[6] This study recognizes that although it is difficult to distinguish between steady state channel profiles predicted by different stream incision rules, each incision rule demonstrates a unique behavior during its transient response to some disturbance [*Howard and Kerby*, 1983; *Stock and Montgomery*, 1999; *Whipple et al.*, 2000; *Whipple and Tucker*, 2002; *van der Beek and Bishop*, 2003]. To evaluate the real-world applicability of any particular incision rule, it thus becomes necessary to compare the predicted transient response with field observations from a disequilibrium landscape with a known age and type of disturbance. The direct comparison between modeled and observed transient landscapes thus provides an excellent opportunity to recognize the strengths and weaknesses of the present formulations for stream incision (Figure 1).

[7] In this paper, we provide a comparative analysis of how four different stream incision rules respond to two different scenarios for base level fall. Two of the four incision rules are simplified versions of two recent sediment flux–dependent incision rules [*Sklar and Dietrich*, 1998; *Parker*, 2004; *Sklar and Dietrich*, 2004; *Gasparini et al.*, 2006; *Gasparini et al.*, 2007]. For reference, we also model the channel response to base level fall using the detachment-limited stream power incision rule [e.g., *Howard and Kerby*, 1983; *Whipple and Tucker*, 1999] and a simplified transport-limited incision rule [*Willgoose et al.*, 1991; *Paola et al.*, 1992a; *Tucker and Bras*, 1998].

[8] Because the incision rate in three of the four studied incision rules is directly dependent on sediment flux, we find it advantageous to employ CHILD [*Tucker et al.*, 2001a, 2001b], a two-dimensional landscape evolution model (Figure 1d) wherein changes in sediment production and transport capacity are explicitly accounted for during the transient response [*Gasparini et al.*, 2006, 2007]. In this study we use a landscape evolution model to examine the interaction between an incising trunk stream and tributary channels with a range of drainage areas.

[9] The two base level fall scenarios modeled here represent end-members for the range of forcing an incising river may experience in response to a sudden, but finite pulse of base level fall. *Gasparini et al.* [2007] considers primarily main stem response to a sustained increase in the rate of rock uplift (or base level fall), as opposed to the finite base level fall events considered here. Our two base level fall scenarios help evaluate the relative sensitivities of the four incision models to the type of base level fall and allow us to mimic the behavior of smaller tributary networks nested within a larger catchment. In the first scenario, we subject the modeled catchment to an instantaneous drop in base level at its outlet. In order to provide comparison to typical field settings (including the Waipaoa River basin, introduced earlier), we elect to drop base level 50 m or ~1/3 of the modeled basin's steady state fluvial relief. For example, instantaneous base level fall could result from stream capture or surface rupture along a fault [e.g., *Sklar et al.*, 2005]. In the second scenario, we examine the response of the river network following a finite but prolonged period of base level fall. In this scenario, we impose a 10 fold increase in the rate of base level fall and allow the model to run until the accumulated base level fall is equivalent to the magnitude of the instantaneous drop in base level (50 m, Table 1). This type of disturbance could result from sea level fall over the shelf slope break [e.g., *Snyder et al.*, 2002] or a temporary increase in rock uplift rate. This scenario also serves to simulate the base level fall signal a subcatchment nested within a larger basin might experience if the outlet to the larger basin was subjected to an instantaneous base level fall.

[10] We begin our analysis by introducing the four stream incision rules utilized here and discussing the simplifications we made to these rules that allow us to write analytical solutions. We then outline the dependence of each model's incision rate on local stream gradient and discuss the

presence or absence of theoretically predicted instabilities. After a brief discussion of the utility and mechanics of the CHILD model, we present, for each of the four incision rules, the transient response of the trunk and tributaries following the two base level fall scenarios. Our subsequent discussion focuses on the interaction between trunk stream incision and the development of hanging tributary valleys.

3. Stream Incision Rules

[11] Our primary motivation is to understand the transient response to base level fall of channels governed by sediment flux–dependent bedrock incision rules. For comparison, we also provide an analysis of the transient response to base level fall of channels governed by the detachment-limited stream power incision rule and a simplified transport-limited stream incision rule. This comparative analysis emphasizes the unique attributes and sensitivity of the sediment flux–dependent incision models. In the following section, we introduce all four of the stream incision rules employed in the CHILD landscape evolution model.

[12] In all cases, we model the potential development of extremely steep channel reaches. Under these conditions, the small-angle approximation, (where $\sin(\alpha) \approx \tan(\alpha)$ and α denotes the bed angle in radians), is no longer valid. In this analysis, we take considerable care to avoid the small-angle approximation. In all equations in this text, the variable S represents $\sin(\alpha)$, not channel gradient. In all figures, however, we transform $\sin(\alpha)$ to the more intuitive variable, channel gradient ($\tan(\alpha)$), using the relation, Gradient = tan(arcsin(S)).

3.1. Transport-Limited and Stream Power Incision Rules

[13] We only briefly discuss the transient behaviors of the transport-limited and the detachment-limited stream power incision rules as these have been well explored by other workers [e.g., *Howard and Kerby*, 1983; *Willgoose et al.*, 1991; *Whipple and Tucker*, 1999, 2002]. In this analysis, we use a simplified rule for transport-limited incision where the volumetric sediment transport capacity is a power law function of unit stream power. This model follows the general form of many other sediment transport equations [*Meyer-Peter and Mueller*, 1948; *Wilson*, 1966; *Fernandez Luque and van Beek*, 1976] where the volumetric sediment transport capacity, Q_t is a power law function of the stream's excess shear stress:

$$Q_t \propto W(\tau - \tau_c)^{3/2}, \tag{1}$$

where W is channel width, τ is the basal shear stress and τ_c is the critical shear stress. All calculations of channel width in this paper (both in analytical and numerical analysis) utilize a power law relation between width and discharge, $W = k_w Q^b$, and a power law relationship between water discharge and drainage area, $Q = k_q A^c$. Combined, these two equations describe the relation between width and drainage area as $W = k_w k_q^b A^{bc}$. Assuming uniform, steady flow in a wide channel and utilizing the Darcy-Weisbach flow resistance equation [e.g., *Tucker and Slingerland*, 1996], shear stress can be expressed as a power law function of upstream drainage area, A, and the sine of the bed angle, S:

$$\tau = k_\tau A^{1/3} S^{2/3}, \tag{2}$$

where k_τ is a constant term characterizing fluid properties, bed morphology and basin geometry. As detailed in previous work [*Willgoose et al.*, 1991; *Paola et al.*, 1992b; *Tucker and Slingerland*, 1997; *Gasparini et al.*, 2007], we assume a negligible threshold of motion for the floods of interest ($\tau \gg \tau_c$) and substitute equation (2) in equation (1), allowing us to write Q_t as a power law function of the upstream drainage area and the sine of the bed angle, $Q_t \propto k_w k_\tau^{3/2} A^1 S^1$, or in a generalized form:

$$Q_t = K_t A^{m_t} S^{n_t}, \tag{3}$$

where K_t is a dimensional coefficient describing the transportability of the channel sediment and m_t and n_t are dimensionless positive constants. Although a critical shear stress could easily be added to numerical simulations (and would importantly influence equilibrium channel slope at low rates of relative base level fall), we retain this simplified form in order to derive analytical solutions that provide considerable insight into the problem addressed here: how, why, and where fluvial hanging valleys form. Under the conditions that lead to hanging valley formation, the assumption that $\tau \gg \tau_c$ is reasonable. We hold $n_t = 1$ in all simulations, consistent with most relations for bed load transport where Q_t is proportional to basal shear stress to the 3/2 power [e.g., *Whipple and Tucker*, 2002, equation (5)]. Given that the change in elevation is a consequence of the difference between the rate of base level fall, U, and the downstream divergence of sediment flux, we can solve for how incision rate varies as a function of S or $\sin(\alpha)$,

$$\frac{dz}{dt} = U - \left(\frac{1}{1-\lambda_p}\right)\frac{d}{dx}\left[\frac{1}{W}\left(K_t A^{m_t} S^{n_t}\right)\right], \tag{4}$$

where λ_p is the sediment porosity and W is the channel width. The effects of a shear stress threshold on channel concavity can be mimicked by increasing the value for m_t and appropriately adjusting K_t, as first proposed by *Howard* [1980]; m_t could reasonably vary between 1.0 and 1.5, and in all of our experiments we set $m_t = 1.5$ (Table 1). Given the form of the incision relation formulated above and $n_t = 1$, the incision rate at a particular drainage area is a linear function of the sine of the bed angle (Figure 2 and Table 1). Because this incision relation has the form of a nonlinear diffusion equation, an oversteepened reach created by base level fall is expected to decay rapidly as it propagates upstream.

[14] The stream power incision rule assumes that transport capacity well exceeds the imposed sediment load and thus the rate of channel incision is limited simply by the channel's capacity to detach bedrock from the channel bed [e.g., *Howard and Kerby*, 1983; *Whipple and Tucker*, 1999]. In this relation, there is no explicit functional dependence of the incision rate on the sediment flux. Changes in bed

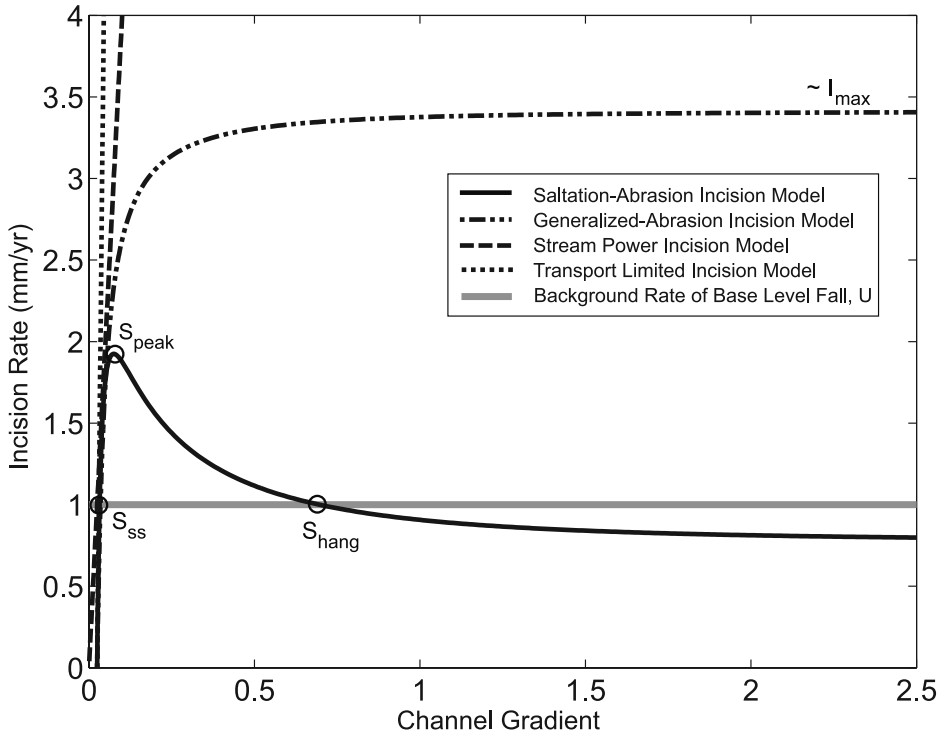

Figure 2. We demonstrate the dependence of incision rate on channel gradient for four channel incision rules. Each line is for a fixed drainage area (1×10^6 m^2) and sediment load. All calculations are made without applying the small-angle approximation. Instead of plotting the x axis with $\sin(\alpha)$, we transform this term to channel gradient, $\tan(\arcsin(\sin(\alpha)))$. The parameters for each of the models are the same as those used in the numerical simulations presented later in the paper. As this figure illustrates, the parameters for each of the models were chosen in order to produce similar steady state slopes ($S_{ss.}$). For both the stream power and the transport-limited models, incision rate increases rapidly with gradients. In the saltation-abrasion model, incision rate initially increases with increasing gradient, exceeding the background rate of base level fall at S_{ss}. After reaching a maximum at S_{peak}, the incision rate monotonically decreases with increasing gradient, eventually dropping below the background base level fall rate (the gray horizontal line) at S_{hang}. The incision rate in the generalized abrasion model initially increases rapidly with gradient and levels off as it asymptotically approaches a maximum incision rate at $I_{\max}$.

elevation are determined by differencing the background rate of base level fall, U, and the bedrock incision rate. The bedrock incision rate is a power law function of A, the upstream drainage area, and S, the sine of the bed angle:

$$\frac{dz}{dt} = U - K_{SP} A^m S^n, \tag{5}$$

where K_{SP} is a dimensional coefficient describing the erodibility of the channel bed as a function of rock strength, bed roughness and climate, and m and n are dimensionless positive constants.

[15] This relation can be rewritten into the same functional form as used to describe kinematic waves [*Rosenbloom and Anderson*, 1994]. As a consequence, base level fall signals modeled with the stream power incision rule propagate upstream through the network as discrete waves. The form of the oversteepened reach may evolve as it propagates upstream depending on the value of n [*Weissel and Seidl*, 1998; *Tucker and Whipple*, 2002]. In this work we utilize unit stream power and assume $m = 0.5$ and $n = 1$ [e.g., *Whipple and Tucker*, 1999]. This results in waves that propagate upstream without changing form and as with the transport-limited model, defines a linear dependence of the incision rate (at any given drainage area) on $\sin(\alpha)$ (Figure 2).

3.2. Sediment Flux–Dependent Models for Channel Incision

[16] Sediment flux–dependent incision rules introduced by *Sklar and Dietrich* [1998, 2004], *Whipple and Tucker* [2002] and *Parker* [2004] explicitly model the dual role of sediment in bedrock channel incision. In these incision rules, when sediment flux exceeds transport capacity, sediment covers and armors the bed against incision and forces the channel toward a transport-limited behavior. For low volumes of sediment flux, insufficient tools are available to impact and abrade the channel bed and results in conditions that approach the detachment-limited state.

[17] In this analysis, we distinguish two classes of sediment flux–dependent incision rules: one where saltation dynamics (on a planar bed) plays a fundamental role in channel incision and another where although incision is similarly accomplished by abrasion alone, saltation dynamics are not explicitly modeled. These models are derived

through minor simplifications of existing sediment flux–dependent river incision models proposed by *Sklar and Dietrich* [1998, 2004] and *Parker* [2004]. Our simplifications facilitate analytical exploration and provide direct comparison to the behavior of previously discussed incision rules [e.g., *Gasparini et al.*, 2006]. Our simplified formulations very closely approximate the behavior of the original equations.

3.2.1. Saltation-Abrasion Incision Rule

[18] The incision rule developed by *Sklar and Dietrich* [1998, 2004] provides a process-specific, mechanistic relation for bedrock incision by the abrasion of saltating bed load of a single grain size on a planar bed. In their rule, the incision rate is an explicit function of both the flux of kinetic energy normal to the bed (impacts) and the fraction of the bed exposed to those impacts. The incision rate for this model, I_{SA}, is written as the product of three measurable terms [*Sklar and Dietrich*, 2004, equation (1)]: the volume of rock prepared for transport per particle impact, V_i, the rate of particle impacts per unit area, per unit time, P_r, and the fraction of the channel's bedrock bed exposed to incision, F_e:

$$I_{SA} = V_i P_r F_e. \tag{6}$$

Each term in this expression can be expanded and expressed as a function of excess shear stress. *Sklar and Dietrich* [2004, equation (24a)] combine the three terms above into a simple expression for bedrock incision. In this analysis, we use their equation (24b), applicable at moderate transport stages ($1 < \tau^*/\tau_c^* < 10$) in which the term representing the influence of incipient suspension is removed. We write their equation (24b) in a form analogous to their equation (24a):

$$I_{SA} = \left[\frac{R_b g}{25\varepsilon_v}\right] \cdot \left[\frac{Q_s}{W}\left(1 - \frac{Q_s}{Q_t}\right)\right] \cdot \left[\left(\frac{\tau^*}{\tau_c^*} - 1\right)^{-0.52}\right], \tag{7}$$

where R_b is nondimensional buoyant density of the sediment, g is gravitational acceleration, ε_v is the energy required to erode a unit volume of rock, Q_s is volumetric sediment flux, W is channel width, Q_t is volumetric sediment transport capacity, τ^* is nondimensional shear stress and τ_c^* is nondimensional critical shear stress. Equation (7) only applies to net erosional settings where Q_s is less than or equal to Q_t. The dual role of sediment flux in determining incision rate is apparent in the second term of equation (7) where as the sediment flux term, Q_s, goes to zero, so does I_{SA}. In contrast, as Q_s approaches the transport capacity, Q_t, then incision rate again goes to zero as the channel bed becomes fully covered with sediment. During the transient response, sediment flux can vary dramatically through time and throughout the basin as hillslopes and tributaries respond to changes in the elevation of the trunk stream. The negative exponent on the third term, excess transport stage, is a consequence of the explicit inclusion of saltation dynamics and determines that incision rate decreases with increasing excess bed shear stress, all else held equal. Using linear regression analysis, we find that the excess transport stage can be reasonably approximated as a power law function of dimensional shear stress and critical shear stress. In order to allow an analytical solution, we further approximate the shear stress exponent as -0.75 rather than the -0.88 value found through this empirical regression analysis:

$$\left(\frac{\tau^*}{\tau_c^*} - 1\right)^{-0.52} \approx 2\left(\frac{\tau^*}{\tau_c^*}\right)^{-0.88} \approx 2\left(\frac{\tau}{\tau_c}\right)^{-0.88} \approx 2\left(\frac{\tau}{\tau_c}\right)^{-0.75}. \tag{8}$$

We find that this approximated form of the excess transport stage term provides a reasonably strong fit to their empirical data as well. Substituting the final term from this approximation back into the third term in equation (7), we can rewrite that expression as

$$I_{SA} = \left[\frac{2R_b g \tau_c^{0.75}}{25\varepsilon_v}\right] \cdot \left[\frac{Q_s}{W}\left(1 - \frac{Q_s}{Q_t}\right)\right] \cdot (\tau)^{-0.75}. \tag{9}$$

We then substitute equation (2) for the shear stress term and move the k_τ term into the first bracketed term in equation (9). In this final expression, which we generically refer to as the saltation-abrasion incision rule, we group the terms in the first bracket of equation (9) as constants that characterize the channel's erodibility, K_{SA}. Following [*Whipple and Tucker*, 2002], we also define the two terms in the second bracket as $f(Q_s)$, an expression reflecting the role of sediment flux in setting the incision rate:

$$f(Q_s) = \frac{Q_s}{W}\left(1 - \frac{Q_s}{Q_t}\right). \tag{10}$$

The first term in this second bracket, (Q_s/W), quantifies the volume of sediment per unit width available as tools. The value for the Q_s term is the sediment supply at a particular point in time and space. Under equilibrium conditions, Q_s is equal to the upstream drainage area times the rate of base level fall (or rock uplift) times the fraction of sediment delivered to the channel as bed load (β). As discussed earlier, width is assumed to be a power law function of drainage area (see section 3.1). The second term, $(1 - (Q_s/Q_t))$, describes the cover effect, where increasing sediment flux relative to transport capacity diminishes the incision rate. The form of the transport capacity is defined above in equation (3). When the sediment flux surpasses the transport capacity, sediment is deposited and equations (9) and (10) are no longer physically valid. The final expression for our saltation-abrasion rule shares the same functional form as the generic sediment flux–dependent incision rule presented by *Whipple and Tucker* [2002, equation (1)], but instead uses significantly different values for the exponents on drainage area and slope:

$$I_{SA} = K_{SA} f(Q_s) A^{-1/4} S^{-1/2}. \tag{11}$$

As we will address in subsequent sections, the negative exponent on S, the sine of the bed angle, exerts an important influence on the responses of tributaries during a transient period of incision and reflects the explicit inclusion of saltation dynamics over a planar bed. When addressing the relationship between incision rate and channel gradient (Figure 2), it is important to recognize that equation (11) has two gradient-dependent terms: first the Q_t term within $f(Q_s)$ is dependent on the sine of the bed angle (see equations (3)

and (10)) and second, the sine of the bed angle term, S, with the negative exponent that occurs following the substitution for shear stress (equation (2) into (9)). As Figure 2 demonstrates, we find that the incision rate increases with increasing channel gradient to a maximum and then decreases with ever-increasing gradients.

[19] The steady state channel profiles, slope-area relations, and dependence of incision rate on channel gradient for this simplified expression are almost identical to those predicted by the original *Sklar and Dietrich* [2004, equation (24a)] incision rule. The gradient of the channel at large drainage area asymptotically approaches that predicted by the purely transport-limited model. The steady state longitudinal form of the channel deviates from the transport-limited gradient only at small drainage areas in upper reaches of the channel network [*Sklar and Dietrich*, 2006; *Gasparini et al.*, 2007, Figure 1a]. However, under steady state conditions, there is a critical drainage area below which channel gradients become infinite. This critical area, as described in detail by *Gasparini et al.* [2007, equation (27)], is a consequence of two characteristics of small drainage areas: (1) low sediment supply and (2) high gradients. Because incision depends on saltating bed load, these two factors limit the interaction of sediment with the bed, thus limiting incision and the applicability of this model at extremely small drainage areas. It should also be noted that decreasing channel width at low drainage areas may offset the diminishing sediment flux, therefore allowing the channel to maintain a constant sediment flux per unit width. Regardless, the steeper slopes observed at low drainage areas (due to the need to transport sediment at shallow flow depths) result in longer hop lengths for saltating grains and a decrease in the efficiency of incision by bed load abrasion. In the CHILD model, diffusive hillslope processes are responsible for sediment production and transport at drainage areas less than this critical area. We reserve further discussion of the dependence of incision rate on gradient for the proceeding section on model instabilities.

3.2.2. Generalized Abrasion Incision Rule

[20] *Parker* [2004] presents an incision model in which two processes dominate erosion of the channel bed: plucking of bedrock blocks and abrasion by saltating bed load. For the abrasion component, the Parker model employs a simplified version of the incision model of *Sklar and Dietrich* [2004], based on analogy to a model of downstream fining due to a constant coefficient of wear. This simplification was not intended to correct the model of Sklar and Dietrich, but instead to provide comparison with other mechanisms of incision. These comments notwithstanding, the Parker model applied to bed load abrasion alone can be used to highlight the role of specific terms in the formulation of *Sklar and Dietrich* [2004] with respect to the formation of hanging valleys. With this in mind, we focus only on the bed load abrasion process (same method applied by *Gasparini et al.* [2007]). This generalized abrasion (GA) rule facilitates simpler analytical solutions and a more direct comparison between the incision rules of *Parker* [2004] and *Sklar and Dietrich* [2004]. The only functional difference between this generalized abrasion rule and the saltation-abrasion model (equation (11)) is that the exponents on both the drainage area and the sine of the bed angle are equal to zero (recall that the negative exponents in the saltation-abrasion rule reflected details of saltation dynamics over a plane bed that have been dropped in the formulation of this generalized abrasion model):

$$I_{GA} = K_{GA}\frac{Q_s}{W}\left(1 - \frac{Q_s}{Q_t}\right), \tag{12}$$

where K_{GA} is a dimensional constant equal to (r/L_s) where r is the fraction of the particle volume detached off the bed with each collision and L_s is saltation hop length. Note that in order to have a constant incision rate, I_{GA}, at steady state, the $f(Q_s)$ term in equation (12) (everything but the K_{GA}) must be constant. Figure 2 shows that incision rate in this generalized abrasion rule monotonically increases toward a maximum incision rate with increasing values of channel gradient. This behavior is a consequence of the gradient (or sine of the bed angle) term in the equation for the volumetric transport capacity (equation (3)). Like the saltation-abrasion incision rule, the generalized abrasion incision rule predicts that at large drainage areas, the channel gradient is determined by the system's sediment transport capacity. At steady state the generalized abrasion incision rule also predicts a critical drainage area at which channel gradients become infinite as a consequence of low sediment fluxes [*Gasparini et al.*, 2007, equation (32)]. As in the saltation-abrasion incision rule, the generalized abrasion rule's threshold drainage area increases with decreasing values of the dimensional constant, K_{GA} (stronger rocks). Unlike the saltation-abrasion incision rule, the generalized abrasion rule's critical drainage area is insensitive to rate of base level fall (or rock uplift). We reserve further discussion of the dependence of incision rate on gradient for the proceeding section on model instabilities.

4. Predicted Transient Instabilities

[21] There are no transient instabilities in the transport-limited or the stream power incision rules as formulated above. The proceeding section outlines instabilities predicted to occur in the two sediment flux–dependent incision rules. These instabilities provide mechanisms for the formation of temporary and permanent hanging valleys. In each case, we assume that during the initial response to base level fall, changes in sediment flux lag behind the profile adjustment (or $Q_s = Q_{s-initial}$). We justify this assumption by suggesting that the hillslope response (which determines sediment flux) is dependent on the transmission of the incision signal through the network. If this assumption is violated and sediment flux does not lag during adjustment, the instabilities predicted below will underestimate threshold gradients or overestimate threshold drainage areas.

4.1. Instabilities in the Saltation-Abrasion Incision Rule

[22] In Figure 2, we demonstrate that the steady state incision rate predicted by the saltation-abrasion incision rule derived from *Sklar and Dietrich* [1998, 2004] initially increases from extremely small values at low gradients, past the steady state gradient at S_{ss}, to a maximum incision rate at S_{peak}. For gradients greater than S_{peak}, the incision

rate decreases monotonically with increasing gradient, reaching an incision rate equal to the background rate of base level fall (or rock uplift) rate at S_{hang}. The nonmonotonic form of the solid curve in Figure 2 is the basis for the instabilities observed in the saltation-abrasion incision rule.

[23] The first of the two instabilities in the saltation-abrasion incision rule occurs if a channel's gradient exceeds the gradient required for the incision rate to keep pace with the background base level fall rate, S_{hang} (Figure 2). Beyond this critical gradient, the stream can no longer effectively erode the bed at a rate sufficient to keep pace with the background base level fall rate, U. This creates a runaway negative feedback that results in the formation of a permanent hanging valley (a waterfall) in all cases.

[24] Both steady state channel gradient, S_{ss}, and S_{hang} are recognized as two of the three roots of equation (11) when $I_{SA} = U$, where U is the rate of base level fall (Figure 2). We can derive analytical expressions for S_{ss} and S_{hang} by starting with equation (11) and setting $I_{SA} = U$, substituting equation (3) for Q_t and setting $Q_s = \beta AU$ (the steady state sediment flux at a given base level fall rate, where β is the percentage of the eroded material that is transported as bed load). We also use a power law width-discharge relation and a power law discharge-area relation to set $W = k_w k_q^b A^{bc}$ as outlined by *Whipple and Tucker* [1999]:

$$U = K_{SA}\left[\frac{\beta AU}{k_w k_q^b A^{bc}}\left(1 - \frac{\beta AU}{K_t A^{m_t} S^{n_t}}\right)\right] A^{-1/4} S^{-1/2}. \quad (13)$$

The solution for steady state gradients as a function of area is found by setting $n_t = 1$ (as discussed above), making the substitution $x = S^{-1/2}$ thus allowing equation (13) to be rearranged into a relatively simple cubic form,

$$x^3 - S_t^{-1} x = -S_t^{-1}\left(\frac{1}{K'\beta A^{1-bc-1/4}}\right), \quad (14)$$

where we group variables and define S_t as

$$S_t = \frac{\beta U}{K_t} A^{1-m_t}. \quad (15)$$

In the two expressions above, S_t defines the steady state transport-limited gradient [e.g., *Whipple and Tucker*, 2002], $K' = K_{SA}/(k_w k_q^b)$, and the generic cubic form of equation (14) is $x^3 + px = j$. The three real roots of this cubic equation are

$$S_1 = \left(2\sqrt{-\left(\frac{1}{3}p\right)}\cos\left(\frac{\theta + 2\pi}{3}\right)\right)^{-2} \quad (16)$$

$$S_{ss} = \left(2\sqrt{-\left(\frac{1}{3}p\right)}\cos\left(\frac{\theta}{3}\right)\right)^{-2} \quad (17)$$

$$S_{hang} = \left(2\sqrt{-\left(\frac{1}{3}p\right)}\cos\left(\frac{\theta + 4\pi}{3}\right)\right)^{-2}, \quad (18)$$

where θ is defined as

$$\theta = \cos^{-1}\left(\frac{\frac{1}{2}j}{\sqrt{-\frac{1}{27}p^3}}\right). \quad (19)$$

These roots define the three potential values for $\sin(\alpha)$ at which the incision rate is equivalent to the background rate of base level fall (Figure 2). The first root, S_1, is unphysical and is not addressed in Figure 2. The second root, S_{ss}, is a physically meaningful solution that describes the value of $\sin(\alpha)$ at steady state. At this value, the channel exhibits a stable, partially covered bed and can erode and transport material at a rate sufficient to keep pace with the background rate of base level fall (or rock uplift). The third root, S_{hang}, is often, but not always, also physically valid and describes the value of $\sin(\alpha)$ above which the incision rate decreases below the background base level fall rate (Figure 2), facilitating the formation of a permanent hanging valley. Naturally, S_{hang} is only physically meaningful for values between 0 and 1 ($\sin(\alpha) = 1$ for a vertical cliff). At values of $\sin(\alpha)$ higher than S_{hang}, the saltating bed load no longer impacts the bed effectively or frequently enough to maintain a sufficiently high incision rate to keep pace with the background rate of base level fall. Basins upstream of these oversteepened reaches are terminally divorced from the lower reaches unless other processes act to reduce channel gradient. Combining equations (14), (15) and (19) into (18) we can derive the value of $\sin(\alpha)$ at S_{hang} as

$$S_{hang} = \left[2\sqrt{\frac{1}{3S_t}}\cdot\cos\left(\frac{1}{3}\cos^{-1}\left(\frac{-1}{2S_t K'\beta A^{1-bc-1/4}\sqrt{\frac{1}{27S_t^3}}}\right) + \frac{4}{3}\pi\right)\right]^{-2}. \quad (20)$$

As presented in Figure 3, the channel gradient required to form a permanent hanging valley increases with drainage area (the increase in S_{hang} with drainage area is exactly commensurate with the decrease in S_{ss} with drainage area). In large tributaries, there is no physically meaningful solution for S_{hang}, because values predicted by equation (20) exceed unity. As discussed later, this implies that larger tributaries will be able to keep up with a given pulse of main stem incision but smaller tributaries experiencing the same magnitude base level fall signal at their junction with the main stem might not. This determines which tributaries form hanging valleys during periods of rapid base level fall.

[25] The second transient instability associated with the saltation-abrasion incision model creates temporary hanging valleys that fail to keep pace with main stem incision for a period of time, but eventually recover and equilibrate to the main stem. These occur when the transient pulse of incision increases the value of $\sin(\alpha)$ greater than S_{peak}, but less than the previously discussed S_{hang} (Figure 2). We can derive the value for S_{peak} at any particular drainage area by solving for when the change in incision rate with respect to $\sin(\alpha)$

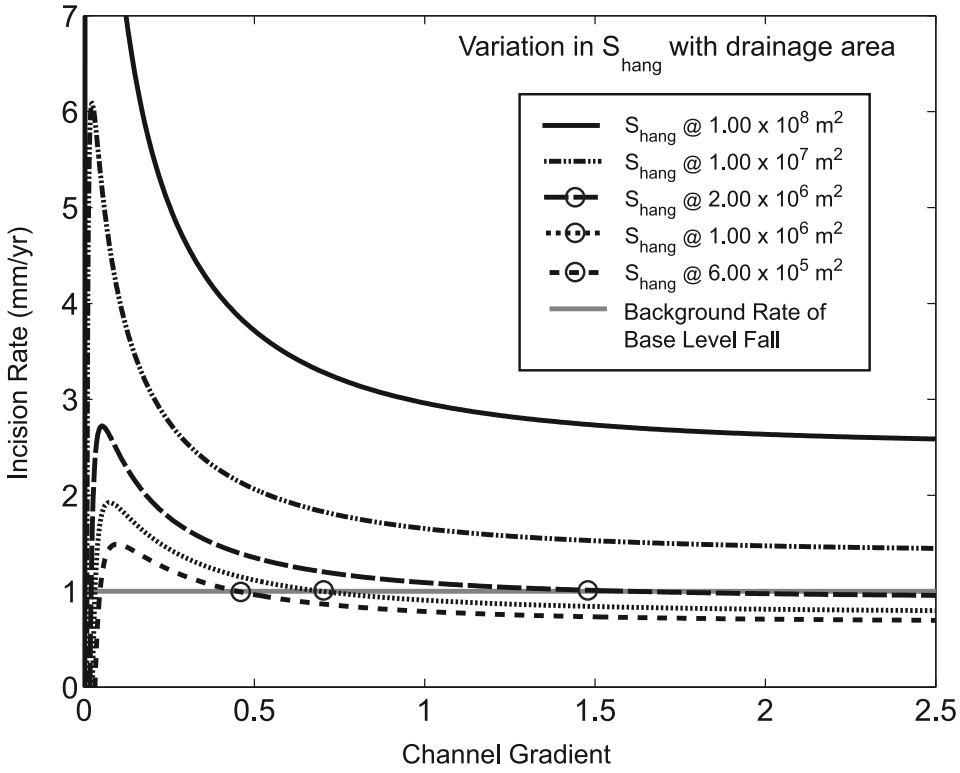

Figure 3. In the saltation-abrasion (S-A) model, the dependence of incision rate on channel gradient varies with drainage area. Note that all calculations were made without applying the small-angle approximation. Instead of plotting the data relative to $\sin(\alpha)$, we plot it relative to a more intuitive variable, channel gradient, $\tan(\arcsin(\sin(\alpha)))$. The gradient at which incision rate falls below the background base level fall rate and permanent hanging valleys form, S_{hang}, decreases with decreasing drainage area. This reveals that small tributaries have a greater probability of creating hanging valleys than large ones. Although difficult to perceive in this figure, the channel gradient at which the S-A model achieves peak incision rates, S_{peak}, increases with decreasing drainage area. Note that drainage basins with drainage areas greater than $\sim 2.5 \times 10^6$ m^2 will never produce permanent hangs from a response to a finite base level fall, indicating that the formation of permanent hangs in these circumstances will only occur at relatively small drainage areas. Tributaries or drainage basins with drainage areas of greater than $\sim 2.5 \times 10^6$ m^2 can only become permanently hung if the incision rate is permanently increased above the maximum incision rate allowable for that drainage area (thus plotting above a given line).

equals zero. We find that this value is three times the initial transport-limited channel gradient or

$$S_{peak} = \frac{3\beta}{K_t} U_{initial} A^{1-m_t}. \quad (21)$$

Because m_t is greater than one (Table 1), the negative exponent on area in equation (21) means that S_{peak} increases with decreasing drainage area. This implies that the difference between S_{peak} and S_{hang} decreases with decreasing drainage area, as does the difference between S_{ss} and S_{hang} (Figure 3). As a result, smaller tributaries are far more susceptible to the formation of permanent hangs than larger tributaries which will either (1) respond quickly in an essentially transport-limited manner or (2) develop a temporary hanging valley and then recover. For an instantaneous pulse of base level fall, a temporary hanging valley forms as the pulse of main stem incision steepens the tributary outlet to values between S_{peak} and S_{hang}. The gradual subsequent incision of this oversteepened reach exceeds the background rate of base level fall, and thus eventually decreases the height and maximum gradient of the oversteepened reach, resulting in a positive feedback loop in which gentler gradients promote greater incision rates and thus more rapid decay of the temporary hanging valley knickpoint. This positive feedback leads to the eventual recovery of the temporary hanging valley to a graded condition. Note that we discuss here only finite episodes of increased base level fall. If accelerated rates of main stem incision were sustained indefinitely owing to a persistent change in rate of base level fall (or rock uplift), permanent hangs would from wherever channels are steepened beyond S_{peak} – this may be the most common circumstance leading to formation of hanging tributaries [*Wobus et al.*, 2006], but is not the case in the Waipaoa field site. In addition, our derivations of S_{peak} and S_{hang} assume we are observing the initial response of the channel (where $Q_s = Q_{s-initial}$); any partial communication of the incision signal to the upper basin will increase sediment delivery and

ultimately increase the predicted values of both S_{peak} and S_{hang}.

4.2. Instabilities in the Generalized Abrasion Incision Rule

[26] Unlike the saltation-abrasion incision rule, the generalized abrasion incision rule (adapted from *Parker* [2004]) does not have a hump or discrete maximum value in the relation between incision rate and channel gradient (Figure 2). Although the exponent on S ($\sin(\alpha)$) in equation (12), is zero, there is still a functional dependence on the channel gradient through the Q_t term defined in equation (3). In the generalized abrasion incision model, for a fixed sediment flux, the incision rate increases asymptotically with channel gradient toward a maximum value, $I_{\max}$ (see Figure 2):

$$I_{\max} = \frac{K_{GA}\beta}{k_w k_q^b} A^{1-bc} U_{initial}. \tag{22}$$

This asymptotic approach to $I_{\max}$ prevents the incision rate from ever declining below the background rate of base level fall in response to channel steepening. The only way the channel could therefore create a permanent hanging valley (or waterfall) would be in the unlikely case where the sediment flux in the upper basin decreases to zero or if base level fall (or rock uplift) was maintained indefinitely at a rate exceeding $I_{\max}$.

[27] Similar to the saltation-abrasion model, in response to a finite period of increased base level fall temporary hanging valleys will form in the generalized abrasion incision rule if the transient incision rate exceeds the maximum incision rate associated with the initial sediment flux. Solving equation (22) for drainage area, we find the maximum drainage area at which a temporary hanging valley could form

$$A_{temp} = \left(\frac{k_w k_q^b}{K_{GA}\beta} \frac{I_{\max}}{U_{initial}} \right)^{\frac{1}{1-bc}}. \tag{23}$$

Following a pulse of incision, the oversteepened reach at A_{temp} decreases channel gradient because the main stem incision rate returns to just balancing the background rate of base level fall ($U_{initial}$) while the tributary continues to incise at a rate equal to $I_{\max}$, resulting in a progressive decay of hanging valley height and the maximum gradient of the oversteepened reach. In addition, sediment flux from upstream increases in response to the incision, resulting in a positive feedback, accelerating incision of the upper lip of the oversteepened reach. This results in the eventual, if asymptotic, readjustment of the tributary to graded conditions following the transient pulse of incision.

[28] Evidence from the Waipaoa River and experimental studies suggest that through most of the channel network, the base level fall signal experienced at a point along the channel is not a discrete, on/off pulse of incision but rather gradually builds toward a maximum incision rate and then declines [*Gardner*, 1983; *Crosby and Whipple*, 2006; K. Berryman et al., The postglacial downcutting history in the Waihuka tributary of the Waipaoa River, Gisborne District, New Zealand, and implications for tectonics and landscape evolution, manuscript in preparation, 2007, hereinafter referred to as Berryman et al., manuscript in preparation, 2007]. This rise and fall in the wave of incision experienced at a tributary junction allows an initial signal of incision to propagate up into the tributary before the large magnitude incision rate potentially results in the formation of a hanging valley that effectively isolates the tributary from the main stem. This partial communication of the initial incision signal may increase tributary sediment flux enough that when the large magnitude incision rate creates an oversteepened reach, the hanging tributary's elevated sediment flux is sufficient to allow eventual recovery.

5. Numerical Simulations of Transient Landscape Response

[29] We utilize the CHILD numerical landscape evolution model to compare the transient responses of landscapes governed by four different stream incision rules [*Tucker et al.*, 2001a; *Tucker et al.*, 2001b; *Gasparini et al.*, 2007]. The CHILD numerical landscape evolution model provides an explicit accounting of sediment production and transport at every model node, thus offering an excellent tool for exploring the transient response of sediment flux–dependent channel incision rules. Triggered by base level fall, channel incision accelerates sediment delivery from diffusion dominated hillslopes and generates a spatially and temporally complex sediment flux response. During each model run, at any point along the main stem channel the sediment flux fluctuates as a consequence of both the local adjustment of hillslopes and the integrated, upstream network response to the pulse of incision. This unsteady sediment flux response directly impacts the continued fluvial communication of the transient base level fall signal through the system.

[30] Although numerical landscape evolution models are useful for studying the interaction between sediment production, sediment transport and channel incision at the network scale, they also present limitations. In all model runs, we define hillslope erosion only as a diffusive process, where the rate of sediment delivery is controlled by a diffusion coefficient, K_D, and the local hillslope gradient. This limits the hillslope transport processes to creep and rain splash erosion. In our application of the CHILD numerical model, we study the transient response within large basins (1×10^8 m^2) (Figure 1d) and thus use a large node spacing of $\sim$100 m (Table 1). This large node spacing, and the subsequent numerical diffusion, contributes to the progressive decay of the incision signal as it propagates upstream. Although this influences evolution of the form of the transient signal in the stream power incision model (Figures 4e–4h), we are less concerned in the other models. Results from model runs that utilized smaller node spacing were hard to distinguish from the runs at the larger node spacing. As discussed by *Whipple and Tucker* [2002] and *Gasparini et al.* [2006, 2007], large drainage area regions in models using sediment flux–dependent incision rules respond to pulses of incision largely in a transport-limited manner. Because this diminishes the impact of numerical diffusion on the modeling of the sediment flux–dependent incision rules (our main focus), we are confident that numerical diffusion does not limit the findings of this study.

[31] Another unintended consequence of large node spacing is that the instantaneous base level fall at the outlet

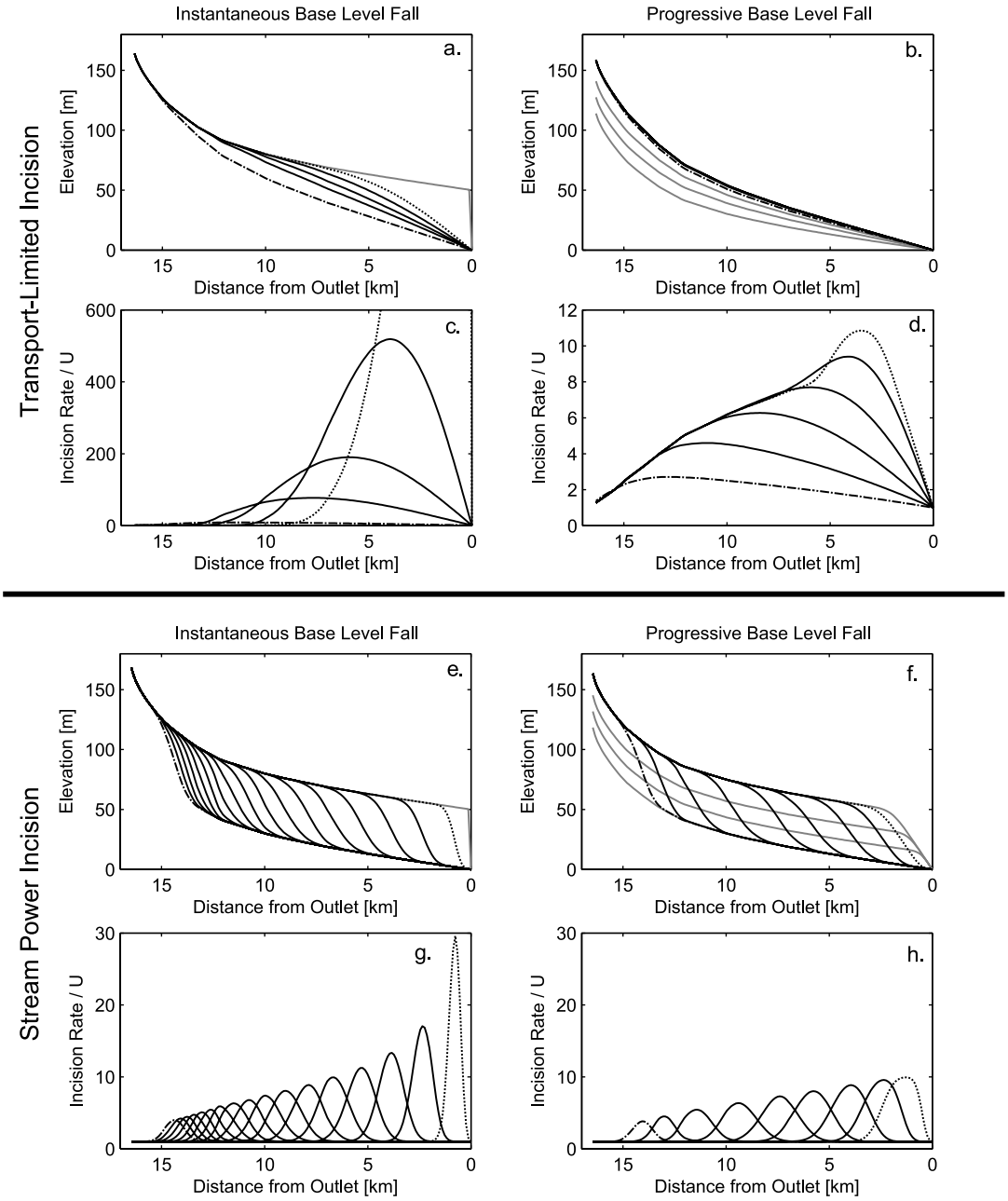

Figure 4. Numerical simulations of main stem profile evolution and normalized incision rates are observed following base level fall. Normalized incision is calculated by dividing the incision rate by the long-term, predisturbance background rate of base level fall. Shown are (a–d) plots that reflect simulations governed by the transport-limited (T-L) incision rule and (e–h) plots that reflect simulations governed by the stream power (S-P) incision rule. In Figures 4a and 4e, the gray line represents the channel profile immediately after the base level fall; the dotted line represents the first profile illustrated after the base level fall; and the dash-dotted line is the final profile illustrated. In Figures 4c and 4g, the dotted and dash-dotted lines illustrate the incision rate for the dotted and dash-dotted profiles in Figures 4a and 4e, respectively. In Figures 4b and 4f, gray lines reveal the evolution of the channel profile during progressive base level fall (no incision rates are shown for these times), and the dotted lines represent the first profile shown after the base level fall rate returns to the background rate; the dash-dotted line is the final profile shown. In Figure 4b, the profile changes very slowly, and therefore the differences between each time plotted are not discernable (plotting times were chosen to show the pattern in incision rate). Note that the y axis differs between Figures 4c and 4d. In each of the plots, the time between each channel profile and incision plot is not necessarily steady; rather, the times plotted were chosen to illustrate the general behavior of the system. Note that the incision signal in the S-P case migrates up the main stem as a discrete step, while in the T-L case, the increase in high sediment delivery during the transient prevents the downstream reaches from reequilibrating.

creates a step whose channel gradient, instead of being a vertical step, is the ratio between the vertical base level fall and the horizontal node spacing. For example, an instantaneous 100 m base level fall on a grid with 100 m node spacing, instead of being near vertical, would have a gradient close to 1 (45 degrees).

[32] In order to test the response of each incision rule to the base level fall scenarios discussed above, we first create four steady state landscapes, each fully adjusted to a particular incision rule. To do this, we start each model landscape as a 10 km by 10 km square of random, low-amplitude topography with a single outlet in one corner and zero-flux edges. Each initial surface is then subjected to uniform and steady rock uplift (or steady base level fall) at the outlet until the network and hillslopes reach equilibrium. These four steady state landscapes provide the initial condition for the base level fall experiments. As we only study the basin's response to finite base level fall, and not a sustained change in the background uplift (or base level fall) rate (as explored by *Gasparini et al.* [2007]), all model parameters are identical before and after the disturbance (Table 1).

[33] For each incision rule, we first examine the responses of the trunk stream to the two base level fall scenarios (as defined in section 2; see Figures 4 and 5). Next, we focus on how the trunk stream's response influences tributary response (Figure 6) as a function of their size and position within the drainage network. The modification of the incision signal as it propagates up the trunk stream provides each tributary with a unique base level fall signal, potentially resulting in significant along-stream variation in tributary response.

5.1. Transport-Limited Channel Incision Rule

[34] The transport-limited incision rule, although computationally expensive in CHILD, is relatively robust over a wide range of parameters (Table 1). Because the transport-limited incision rule is a nonlinear diffusion equation, the oversteepened reach created by the instantaneous base level fall decays rapidly as the convex kink in the channel profile propagates upstream (Figures 4a, 4b, and 6a). As a consequence, the highest incision rates of all four incision models are observed during the initial transport-limited adjustment to instantaneous base level fall. As the base level fall signal propagates upstream, the peak in incision rate moves surprisingly slowly upstream (Figures 4c and 4d). Although the maximum incision rates are extremely high in this model, the location of the peak incision rate does not sweep upstream at the same rate as was observed in the other models. We suggest that this is a consequence of the lower reaches being overwhelmed by the high sediment fluxes generated during transient adjustment.

[35] For the scenario where base level lowers progressively through time (Figures 4b and 4d, gray lines), much of the channel network efficiently steepens as the transport-limited channel responds to the temporarily higher rate of base level fall. No distinct knickpoints are created along the channel profile (Figure 4b). Once the rate of base level fall returns to the lower background value, a diffuse pulse of incision sweeps up the main stem channel and slowly decreases the channel gradient of the transiently oversteepened channels (Figures 4d and 6b). As in the instantaneous base level fall example above, the highest incision rates occur near the outlet and progressively diminish as the signal translates upstream.

[36] The response of the landscape to the two base level fall scenarios is very similar and it could be argued that the instantaneous fall scenario, after a number of time steps, closely resembles the initial form of the progressive base level fall scenario. The only significant difference between the two cases is that the response in the progressive base level fall model is slightly faster than the response to an instantaneous base level fall. Neither of the two models creates temporary or permanent hanging valleys during the transient response. The only delay in response is a consequence of the lag in hillslope sediment delivery following the pulse of incision.

5.2. Stream Power Incision Rule

[37] The detachment-limited stream power incision rule runs much more efficiently than any of the other incision rules in CHILD because sediment flux does not need to be explicitly accounted for at every node. The CHILD model is relatively robust to the parameters chosen for the stream power incision rule (Table 1). As discussed above and expanded upon below, the only limitation of modeling the stream power incision model in CHILD is that numerical diffusion rapidly attenuates the sharp breaks in channel gradient that should persist during the transient response (Figures 4e–4h).

[38] For conditions where $n = 1$ and absent any numerical diffusion, the transient response following instantaneous base level fall should resemble a shock wave where the imposed step in the channel profile retreats upstream with out changing form or magnitude. For values greater than or less than one, the form of the step is modified as it retreats upstream [*Weissel and Seidl*, 1998; *Tucker and Whipple*, 2002]. In the CHILD model, the step propagates upstream (Figure 4e) at a rate that is a power law function of drainage area [*Rosenbloom and Anderson*, 1994], and slows stepwise at tributary junctions but never creates permanent or temporary hanging valleys (Figure 6c) [see also *Niemann et al.*, 2001]. In the stream power model, the transient signal propagates throughout the entire extent of the channel, reaching the headwaters without ever forming a hanging valley.

[39] During progressive base level fall (Figures 4f, 4h, and 6d), near the outlet, the channel steepens to a higher gradient appropriate to the temporarily higher base level fall rate. Once the period of rapid base level fall ends, the oversteepened reach propagates upstream in the same manner as the discrete step did in the instantaneous base level fall scenario. The oversteepened reach maintains the form of a steady state channel segment adjusted to the higher rate of base level fall as it migrates upstream, so long as $n = 1$. Just as with the instantaneous base level fall, in the numerical simulations the oversteepened reach is modified during its upstream migration as a consequence of numerical diffusion. For tributaries, the differences between the instantaneous and prolonged base level fall responses are insignificant (Figures 6c and 6d).

5.3. Saltation-Abrasion Incision Rule

[40] Both the steady state form and transient response of CHILD landscapes governed by the saltation-abrasion

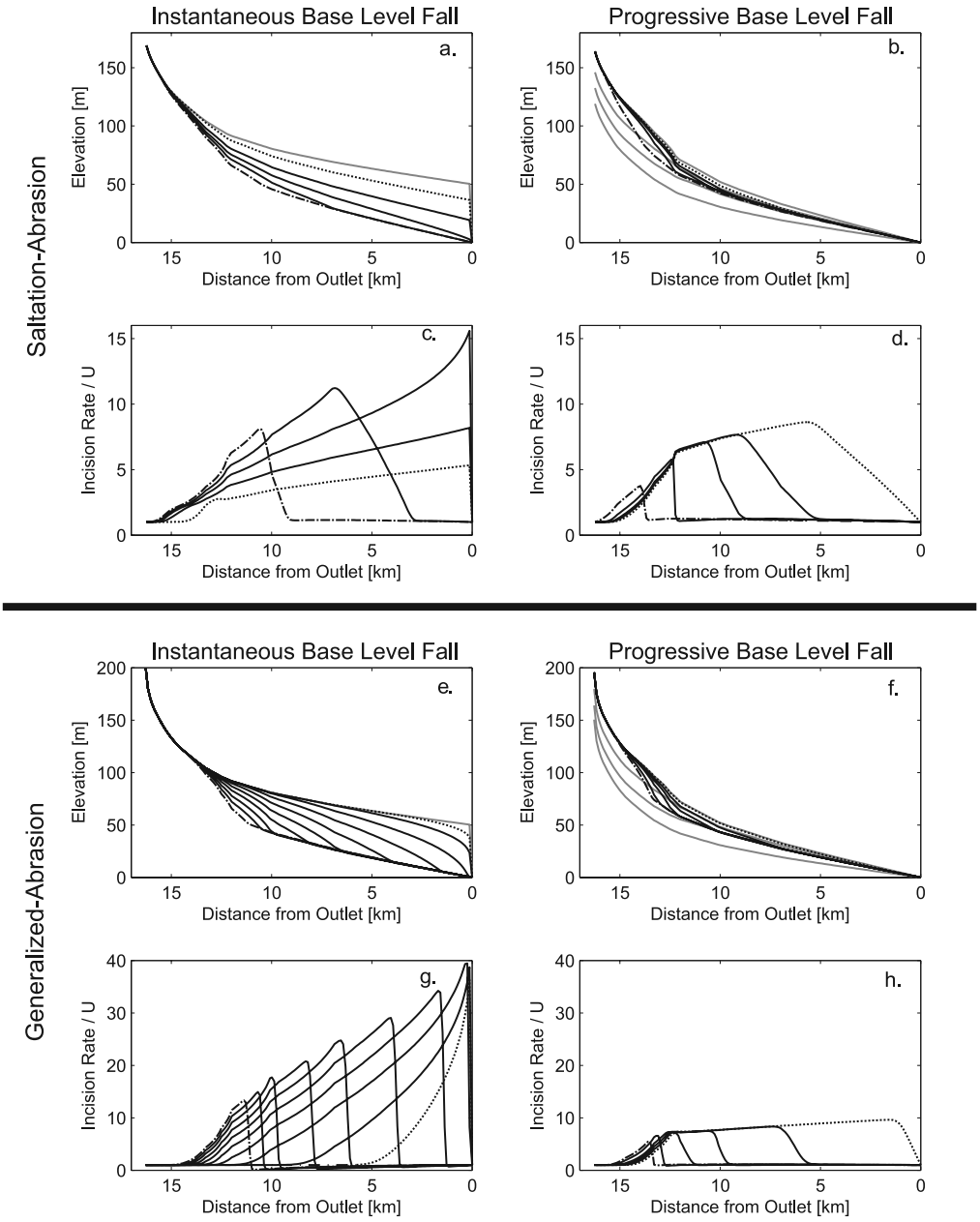

Figure 5. (a–h) Numerical simulations of main stem profile evolution and normalized incision rates are observed following base level fall. Plots illustrate the initial transient response following disturbance, not the full reestablishment of steady state channel form. Note that in each plot, the times between curves are not necessarily equal. In the plots illustrating profile and incision rate response to an instantaneous base level fall (Figures 5a, 5c, 5e, and 5g), the gray lines indicate the profile immediately after the base level fall; the dotted lines indicate the first time step illustrated after the base level fall, and the dash-dotted lines indicate the last time step illustrated. In the plots illustrating the profile and incision rate response to progressive base level fall (Figures 5b, 5d, 5f, and 5h), the gray lines show the evolving profile during progressive base level fall; the dotted lines indicate the first time step after the progressive base level fall; and the dash-dotted lines indicate the final time step illustrated. Figures 5a–5d reflect simulations governed by the simplified saltation-abrasion (S-A) incision rule, while Figures 5e–5h reflect simulations governed by a generalized abrasion (G-A) incision rule. In Figures 5a and 5c, instantaneous base level fall creates high-outlet gradients (between S_{peak} and S_{hang}) in the S-A model and initially retards the upstream transmission of the full incision signal. In Figures 5b and 5d, progressive base level fall in the S-A model creates an oversteepened channel (with gradients between S_{ss} and S_{peak}) that rapidly readjusts toward its predisturbance form. Figures 5e and 5g demonstrate the rapid decay (at I_{max}) of the step created by instantaneous base level fall in the G-A model. In Figures 5f and 5h, the response following the disturbance is fast, but maximum incision rates are limited by the maximum channel gradients created by the progressive base level fall.

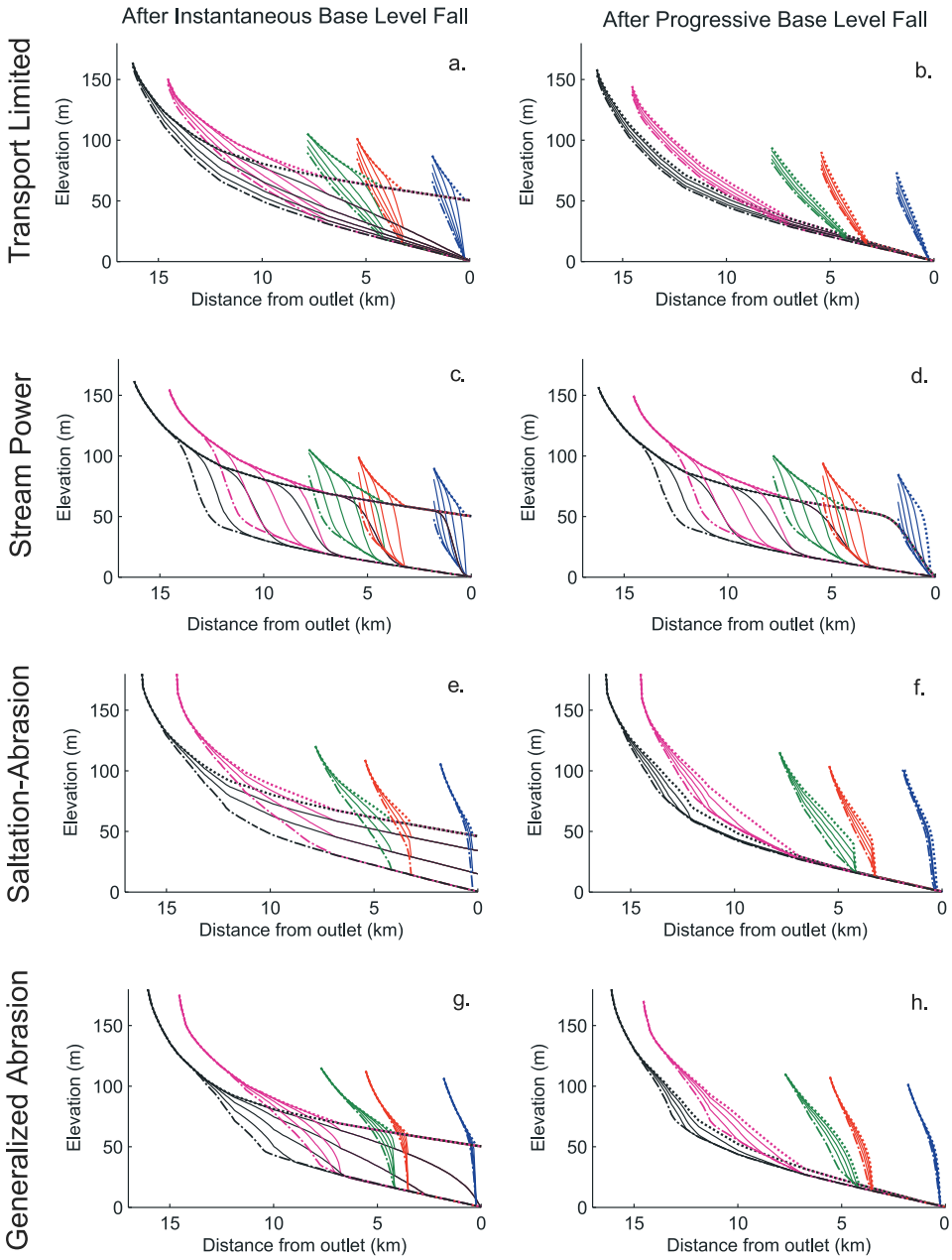

Figure 6. (a–h) Numerical simulations of tributary profile evolution are observed following base level fall. In all plots, the dotted line indicates the profile after the first time step of adjustment, and the dash-dotted profile indicates the last time step illustrated. In Figures 6a and 6b, tributaries in the transport-limited model adjust in concert with incision in the main stem, never developing hanging valleys. Figures 6c and 6d demonstrate that in the stream power model, a wave of steepening and high incision rates sweeps up the main stem and through the tributaries. Tributaries initially steepen in proportion to the main stem as set by their drainage areas but then rapidly relax. Hanging valleys do not form. Figure 6e demonstrates that for instantaneous base level fall in the saltation-abrasion model, the oversteepened reach locally diminishes the incision rate at the outlet. This buffers the rapid upstream communication of the base level fall signal. Upstream tributaries consequently experience slow main stem incision rates and thus never create permanent hanging valleys. Figures 6f, 6g, and 6h demonstrate the formation of temporary hanging tributary valleys as the pulse of incision rapidly migrates up the main stem. In these plots, the behavior of the tributary closest to the outlet, which has the smallest drainage area, is notably different from the evolution of the other tributaries. Note that in all of the plots, the times between curves are not necessarily equal.

incision rule are highly sensitive to the parameters used. Modeled landscapes with realistic channel gradients and network densities are created only by a narrow combination of values for hillslope diffusivity, K_t and K_{SA} (Table 1). This sensitivity is a direct consequence of the inclusion of saltation dynamics in the model (and thus the negative exponents on drainage area and $\sin(\alpha)$, equation (11)).

[41] When subjected to a 50 m instantaneous base level fall (Figure 5a), the discrete step created between the first and second nodes of the main stem fails to retreat. As the model runs forward in time, the step, locked in position at the outlet, very slowly begins to decrease elevation. For each increment of lowering at the top of the step, the small incision signal is rapidly transmitted through the upper portion of the basin (Figures 5c and 6e). The reason the step fails to retreat and instead slowly lowers is because the channel gradient created by the 50 m base level fall lies between S_{peak} and S_{hang} on the plot of incision rate versus gradient (Figures 2 and 3, solid lines). If the magnitude of base level fall were extreme, the resulting channel gradient at the outlet would exceed S_{hang} (Figure 3). In this scenario, the incision rate in the oversteepened reach would drop below the background rate of base level fall and the entire network would be permanently hung above the outlet (a result confirmed in several simulations not reported here). For instantaneous base level falls significantly less than 50 m (given our 100 m cell size) the channel gradient at the outlet is smaller and closer to S_{peak} and consequently the step degrades faster than for larger base level falls. For larger base level falls, the knickpoint remains at the outlet. During each time step, a small fraction of the knickpoint's height is able to propagate upstream. These incremental base level fall signals are too small to create steep slopes or hanging valleys in any tributary upstream (Figure 6e). We found it impossible for an instantaneous base level fall event to create a temporary or permanent hanging tributary using the saltation-abrasion incision model, except at the basin outlet itself. This reflects mostly the restricted size of drainage basins we can simulate with the moderate resolution of 100 m cells. If we consider that the modeled basin is analogous to a tributary within a much larger drainage basin, an instantaneous base level fall at the outlet of the much larger basin would create a progressive base level fall at the outlet of our simulated catchment; a scenario we consider next.

[42] For progressive base level fall (Figures 5b, 5d, and 6f), only moderate gradients develop at the outlet. Because these moderate values of $\sin(\alpha)$ never exceed S_{peak}, there is a rapid upstream propagation of the base level fall signal without ever creating a permanent or temporary hanging valley at the basin outlet. If the prolonged main stem base level fall produces a value of $\sin(\alpha)$ at the outlet that is close to S_{peak}, then the main stem channel incises at its maximum potential rate, propagating the incision signal rapidly through the network. During progressive base level fall, rapid incision in the main stem can create tributary gradients in excess of their local S_{hang} or S_{peak}, resulting in the formation of permanent or temporary hanging valleys (Figures 7 and 6f, respectively). For slower rates of progressive base level fall, the value for $\sin(\alpha)$ at the outlet is significantly less than S_{peak} and the transient signal propagates quickly through the network without forming hanging tributaries except in the smallest of tributaries. In Figure 6f we examine the response of the channel network after the base level fall rate has returned to the background rate. Under this circumstance, the node spacing is too large and the magnitude of base level fall is too small to create permanent hanging valleys. All tributaries reequilibrate to the new base level. It is important to note that for all progressive base level fall scenarios, the main stem incision signal decreases in both amplitude and retreat rate as it propagates upstream through the network (Figure 5d). This means upper basin tributaries feel a smaller maximum incision rate for a longer duration. As discussed earlier, S_{hang}, the gradient necessary to create a permanently hanging valley decreases with decreasing drainage area. Although most hanging valleys form lower in the catchment where the main stem incision rate is fast, (by creating channel gradients at junctions in excess of S_{hang}), upper basin tributaries experiencing relatively low main stem incision rates can still form hanging valleys if their drainage area is sufficiently small. These findings are consistent with field observations in New Zealand [*Crosby and Whipple*, 2006] and Taiwan [*Wobus et al.*, 2006].

[43] We can manipulate base level fall rates in the saltation-abrasion model (or the generalized abrasion model) so that the incision rate in the main stem surpasses the maximum allowable incision rate in some or all of the tributaries. In Figure 7, we demonstrate that for different magnitudes of progressive base level ($5\times$, $10\times$ and $15\times$ $U_{initial}$), tributaries of different drainage area can become hung above the main stem during progressive base level fall. The tributaries become elevated above the main stem when their junction is only capable of incision at a rate below the background rate of base level fall. Because the transient base level fall signal is attenuated as it propagates upstream, we observe variations in response at different upstream distances, at different tributary drainage areas and for different base level fall magnitudes.

5.4. Generalized Abrasion Incision Rule

[44] For all CHILD model runs using the generalized abrasion incision rule, permanent hanging valleys never form as a consequence of instantaneous or progressive base level fall, as expected from the analytical solutions discussed above. Relative to model runs using the saltation-abrasion incision rule, landscapes predicted by the generalized abrasion incision rule are much more stable over a wider range of parameter space (utilized values provided in Table 1). In the generalized abrasion incision model, the main stem response to both base level fall scenarios behaves similarly to the channels governed by the transport-limited incision rule (Figures 5e and 5f). The step created by the instantaneous base level fall signal decays quickly as it retreats upstream (Figure 5e). The plot of normalized incision rate shows the decrease in incision rate as the main stem signal decreases gradient as it propagates upstream (Figure 5g). The tributaries (Figure 6g) contain temporary hanging valleys that relax as the upstream end of the oversteepened reach rounds off. By the end of the main wave of adjustment, the channel profile appears to have reached a steady form but it is still steeper than the equilibrium gradient. This is a consequence of the excess sediment flux still being delivered off the adjusting hillslopes. Although the main

stem channel may stabilize, it remains at disequilibrium until all portions (channels and hillslopes) of the landscape return to equilibrium. Contrasting the response to the pulse of incision, this return to equilibrium is a top-down process where the hillslopes have to adjust before the channels complete their adjustment.

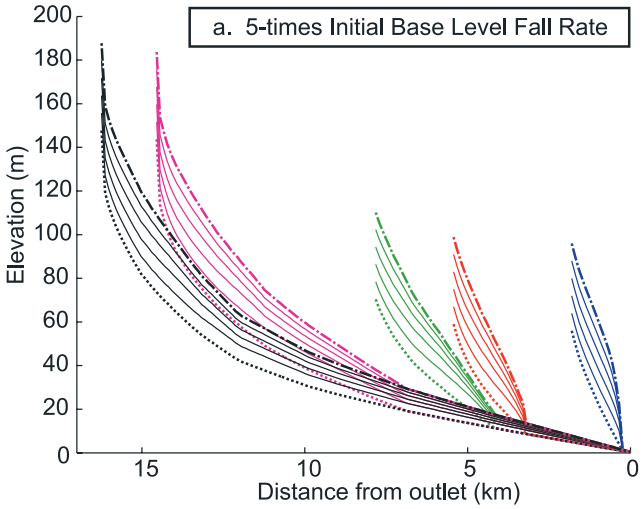

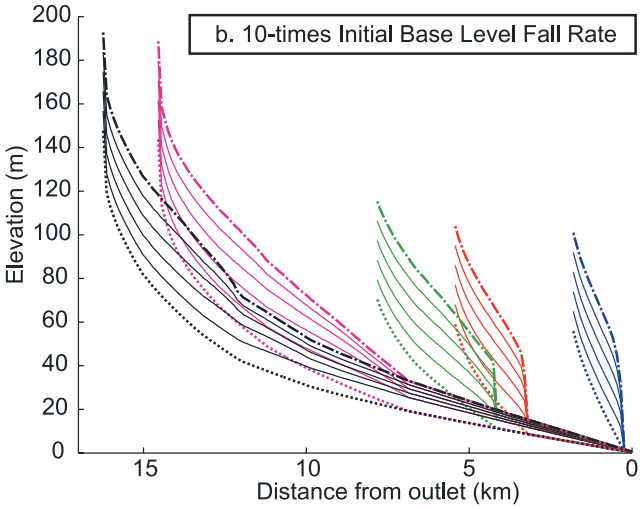

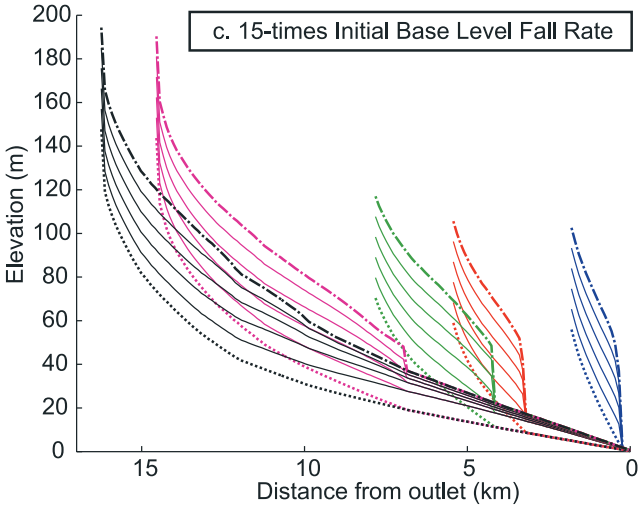

[45] During the period of progressive, accelerated base level fall, the main stem channel rapidly adjusts by increasing channel gradient. When the initial base level fall rate is restored (Figure 5f), the form of the profile resembles that observed halfway through the instantaneous base level fall response (Figure 5e). Because lower reaches of the main stem are graded to the elevation of the outlet, the progressive base level fall scenario more rapidly adjusts back toward steady state. This is reflected in a reduced basin response time and a smaller maximum incision rate (Figure 5h) and the failure to initiate permanent hanging tributaries (as discussed above with respect to Figure 6h).

[46] Temporary hanging valleys do form around A_{temp} in landscapes modeled in CHILD with the generalized abrasion incision rule as a consequence of the lag time in sediment flux delivery from tributary hillslopes (Figure 6g). Without sufficient sediment delivered from upstream, the incision rate at an oversteepened tributary junction decreases and a temporary hanging valley forms. As the tributary's hillslopes increase sediment delivery in response to the initial partial communication of the incision signal upstream of the oversteepened junction, the incision rate in the hanging valley increases. Incision at the lip of the oversteepened reach eventually leads to the decay of the hanging valley and reestablishment of graded conditions.

6. Discussion

[47] Our analytical results and numerical simulations demonstrate that sediment flux–dependent incision rules present viable mechanisms for the formation of both permanent and temporary hanging valleys. In landscapes governed by the two sediment flux–dependent incision rules used here, the progressive modification of the base level fall signal as it propagates up the main stem determines the magnitude and duration of the incision signal at each tributary junction. Lower basin tributaries, located near the outlet where the base level fall initiates, feel the fastest incision rates for the shortest duration and thus have the

Figure 7. Formation of permanent hanging tributaries in the saltation-abrasion model requires sufficiently fast main stem incision rates. This figure examines tributary response given three different rates of progressive base level fall. (a) For 5× the initial base level fall rate, only the two tributaries with the smallest drainage areas (the two closes to the outlet) form a hanging valley. (b) For 10× the initial base level fall rate, all three of the smallest tributaries near the outlet form hanging valleys. (c) For 15× the initial base level fall rate, all tributaries in the basin become hanging valleys. For each hanging tributary, the incision rate in the main stem outpaces the incision rate at the tributary junction. If the progressive base level fall is sustained, the hanging tributaries will increase in elevation indefinitely. Depending on the slopes of the oversteepened reaches ($S_{junction}$), once the base level fall rate returns to the background rate, the tributaries either will remain as permanent hanging valleys (if $S_{junction} > S_{hang}$) or will gradually reestablish grade with the main stem channel (if $S_{junction} < S_{hang}$).

greatest potential to create large drainage area hanging valleys. The pulse of incision is attenuated in a different manner for each incision model as it propagates upstream (Figures 4c, 4d, 4g, and 4h and 5c, 5d, 5g, and 5h), thus upper basin tributaries experience a long-duration signal at a lower incision rate. This upstream attenuation of the main stem incision signal plays an important role in determining whether particular tributaries become either temporary or permanent hanging valleys. In the saltation-abrasion model, our modeling demonstrates that a permanent hanging valley forms when the tributary channel gradient exceeds S_{hang}. This threshold gradient decreases for lower drainage area tributaries (Figure 3). We also demonstrated that the gradients required to form temporary hanging valleys in both the saltation-abrasion and the generalized abrasion incision rules decrease at lower drainage areas. Consequently, following a single pulse of incision, the resulting basin-wide distribution of permanent and temporary hanging valleys is governed by a complicated competition between four main factors: the magnitude of the initial base level fall at the outlet; the rate of upstream attenuation of that incision signal as it propagates up the main stem; the lag time of the sediment flux response and the nonsystematic variation in tributary drainage areas within the channel network.

[48] If the magnitude and duration of the incision signal changes as it propagates upstream, the sediment flux–dependent incision rules suggest that tributaries of identical drainage area at different locations in the basin will not have the same propensity to form hanging valleys. In a study of hanging valleys in the Coast Ranges of Taiwan, *Wobus et al.* [2006] recognize that most hanging tributaries in their field area have a trunk-to-tributary drainage area ratio greater than ~10:1 [*Wobus et al.*, 2006, Figure 11]. Lower in the main stem, our analysis supports the observation that main stem drainage area must be significantly greater than tributary drainage area to create high enough tributary gradients to form hanging valleys. Our analysis also provides evidence that this trunk-to-tributary drainage area ratio for hanging valley formation is sensitive to the four factors listed above, especially in the upper portion of the network where the tributaries and the trunk stream may be of similar drainage area and both close to forming hanging valleys.

[49] Comparing the channel response to both instantaneous and progressive base level fall signals, we find that extending the time of base level fall diminishes the magnitude of the maximum incision rate and extends the duration of the pulse of incision. By distributing the same magnitude main stem base level fall signal over a longer time period, tributary junctions have a greater probability of keeping pace with main stem incision and thus a lower likelihood of creating temporary or permanent hanging valleys. That said, we also recognize that in most field settings, large magnitude instantaneous base level fall events will be significantly less frequent than periods of progressive base level fall.

[50] As anticipated, the transport-limited and detachment-limited stream power incision rules did not generate either permanent or temporary hanging valleys. In these model runs, the base level fall signal was communicated all the way to the headwaters. In the transport-limited model, the response to base level fall was extremely rapid. The only significant lag in channel response was due to overwhelming the channel by high initial sediment fluxes and the delay in hillslope adjustment to the incising streams. The model basin governed by the detachment limited incision rule did not create hanging valleys at tributary junctions that grew in magnitude or slowed the retreat rate any more than anticipated by the celerity model for detachment-limited knickpoint retreat [*Rosenbloom and Anderson*, 1994; *Whipple and Tucker*, 1999; *Crosby and Whipple*, 2006].

6.1. Limitations and Recommendations for Future Work

[51] In future analyses, it would be advantageous to decrease node spacing of the model to limit the effect of numerical diffusion on channel evolution and to allow tributary junctions to steepen above S_{hang}. This could be achieved by running the code on a faster machine or on a cluster or by simply budgeting longer run times for each analysis. Although the CHILD model offers an excellent environment for testing the behavior of sediment flux–dependent incision rules, we recognize that the treatment of hillslope processes requires improvement. With more explicit hillslope erosion processes active, simulation of the rate and magnitude of sediment delivery to the channels following incision would be improved. We also suggest that improved parameterization of hillslope processes will allow hanging tributaries created by thresholds in the sediment flux–dependent incision rules to continue to evolve and retreat upstream because of nonfluvial processes (such as: sapping, mass wasting, weathering, debris flows, etc.), as observed at some field sites [e.g., *Laity and Malin*, 1985; *Weissel and Seidl*, 1997]. In addition, we have not addressed potentially important adjustments in channel width, bed material grain size, and hydraulic roughness.

[52] Future analyses would also benefit from examining the impact of spatially variable substrate erodibility on the attenuation or modification of pulses of incision and the retention or decay of hanging valleys. Adding this dimension to the analysis would bring it closer to representing the field sites we hope to better understand. Along these lines, it would also be advantageous to consider more complicated signals of base level change. For example, how would multiple base level fall events staggered in time influence the sensitivity of tributaries to forming hanging valleys? The predisturbance gradient of a tributary channel is an important factor in determining its sensitivity to a particular base level fall signal. Variations in tributary gradient could occur as a consequence of local lithology in the tributary or as a consequence of incomplete adjustment to a previous transient signal. If the tributary is already oversteepened (but not hanging) from a previous incision event, then it might require a smaller main stem incision event to cause the tributary to hang. A well-adjusted tributary of similar drainage area, sediment flux and position in the network but lower channel gradient would not share the same sensitivity to the smaller magnitude incision event.

6.2. Implications for Landscape Evolution and Field Observations

[53] Analytical and numerical investigations of the response of sediment flux–dependent incision rules to base level fall provide significant evidence for the formation of oversteepened reaches at tributary junctions as a conse-

quence of exceeding threshold gradients. Because modern field observations provide an incomplete record of past events, the utilization of theoretical analyses, as presented above, provide an effective mechanism for testing sparse field data against continuous modeled data. Our work in the Waipaoa River, New Zealand [*Crosby and Whipple*, 2006] and in the Coast Ranges of Taiwan [*Wobus et al.*, 2006] provide useful data sets to compare with modeled behavior.

[54] Numerous characteristics of the modeled behavior align well with our observations from the Waipaoa River basin [*Crosby and Whipple*, 2006]. In this fluvial catchment, a pulse of incision that initiated ~18,000 years ago has lowered base level ~80 m throughout the main channels in the 2150 km^2 basin on the North Island of New Zealand. Some ~236 knickpoints are distributed on tributaries throughout the basin, many of which are positioned at junctions between tributaries and the trunk streams. Although the cause of the pulse of incision is unclear, flights of intermediate fluvial terraces suggest that trunk stream incision was progressive rather than instantaneous. There is also evidence for a gradual rise and then decline in incision rate (Berryman et al., manuscript in preparation, 2007). This evidence for a rise and fall in incision rates fits well with the modeled behavior of sediment flux–dependent incision rules because, even for an instantaneous base level fall signal, the transport-limited nature of these incision rules at large drainage provides a suitable mechanism to attenuate the incision signal.

[55] In the Waipaoa, large magnitude (50–100 m) knickpoints with well defined upstream lips are most frequently found just upstream of tributary junctions, as predicted by both sediment flux–dependent incision models. There are no observations of undercutting plunge pools or cap rock conditions that would facilitate the maintenance of a discrete kink at the knickpoint lip. Field observations suggest that the minor retreat of the oversteepened reaches from the tributary junctions is dominated by nonfluvial processes including physical and chemical weathering, block failures and other mass wasting processes. In both the Waipaoa River and Taiwan, we find that this retreat distance back from the main stem is drainage area–dependent [*Crosby and Whipple*, 2006]. This suggests that though the process of retreat may be nonfluvial, it can still be sensitive to the geometry of the drainage basin. Groundwater processes or the combined contribution of fluvial and nonfluvial processes may contribute toward the retreat and decay of hanging valleys.

[56] In the Waipaoa, the tributary reaches upstream of the knickpoints have two distinguishing characteristics: (1) there is very little incision into either the bed of the hanging tributary or the knickpoint lip and (2) the hanging channels are bare with almost no sediment on planar bedrock beds. The first observation aligns well with the saltation-abrasion model for the case where the oversteepened reach is greater than S_{hang}. Alternatively, the observation could fit well with either the saltation-abrasion model or the generalized abrasion model given the assumption that sediment production in the upper basins decreased dramatically and the hanging valleys have not produced sufficient tools to erode either the channel bed or the knickpoint lip. This is supported by the observation that the hillslopes in many of the broad, flat bottomed hanging valleys only deliver sediment to their foot slopes, not the channel. Extensive fill deposits border the hillslopes, storing the sediment derived from the hillslopes and inhibiting the transfer of material to the fluvial network.

[57] Model simulations provide strong evidence that, for channels governed by sediment flux–dependent incision rules, two mechanisms extend the basin's response time following disturbance. First, because sediment delivery from hillslopes appears to lag behind fluvial incision, the channel's return to equilibrium is prolonged as the hillslopes slowly reestablish equilibrium sediment delivery. The second mechanism that extends the response time is the formation of temporary or permanent hanging valleys in which potentially slower, lithology-dependent, nonfluvial processes may dominate the knickpoint retreat process.

[58] Our simulations also suggest that in noncaprock environments, the concept of a "knickpoint retreat rate" needs to be carefully evaluated as the upstream communication of a pulse of incision is neither continuous nor a process dominated by a single mechanism. Because the relative contribution of different erosion processes will vary as the signal propagates upstream, the measured retreat rates in the main stem may not be able to be extrapolated into the tributaries. Multiple observations of transient features such as terraces and knickpoints provide a basin-wide context to help differentiate between the different styles of signal propagation. Even with this basin-wide context, it is difficult to take locally measured retreat rates and scale them appropriately to constrain the rate of adjustment in basins complicated by network structure and nonuniform substrate.

[59] Further analysis of how tributaries and trunk streams interact will provide not only a better understanding of how rivers communicate signals of incision through their network of streams, but also shed light on the processes that dictate the rate of sediment delivery to depositional basins. Because of the abrupt, large magnitude changes in important parameters such as channel gradient, water discharge and sediment flux, the likelihood of process transitions at tributary junctions complicate the transmission of these signals between trunk and tributary. The development of hanging valleys not only impedes the upstream transmission of subsequent incision signals and delays the equilibration of sediment delivery from hillslopes, but also limits the connectivity of pathways for mobile species such as fish. The loss of this connectivity can segregate and isolate biological communities, potentially affecting species evolution [e.g., *Montgomery*, 2000].

7. Conclusions

[60] We present evidence from both theoretical and numerical analyses that sediment flux–dependent incision rules predict the formation of temporary and permanent hanging valleys in fluvial networks responding to a finite pulse of incision. We find that four factors determine the distribution of hanging valleys in fluvial networks: the magnitude of the pulse of incision; the rate of decay of the incision signal as it propagates upstream; the lag time of the sediment flux response and the drainage area of the tributary. The channel gradients required to create permanent or temporary hanging valleys decrease with decreasing drainage area, thus making it possible for even upper basin tributaries receiving an attenuated base level fall signal to

become hung above the main stem. Although the generalized abrasion incision rule provides mechanisms for the formation of temporary hanging tributaries, the formation of permanent hanging valleys in the saltation-abrasion incision rule provides a better fit to our field observations of both knickpoint form and process transitions at knickpoints. We also suggest that, though the saltation-abrasion incision rule provides a good fit to field data, any incision rule in which the incision rate begins to decline beyond some critical channel gradient will allow the formation of hanging valleys. Therefore an important caveat to our findings is that the formation of fluvial hanging valleys cannot at this juncture be exclusively associated with sediment flux–dependent incision models and thus do not unequivocally demonstrate that these models are correct. Our findings do unequivocally demonstrate some important shortcomings of the standard detachment-limited and transport-limited river incision models that will become important in some applications. For instance, the development of hanging valleys in tributaries extends the response times of landscapes well beyond those predicted by the stream power or transport-limited incision rules. An improved understanding of the erosion processes that modify the oversteepened reaches (or waterfalls) once hanging valleys have formed will improve our predictions of landscape response time and the delivery of sediment to depositional basins.

[61] **Acknowledgments.** The authors wish to thank reviewers Noah Finnegan, Gary Parker, Josh Roering, and Bob Anderson for insightful reviews which considerably improved the clarity of an earlier version of this manuscript. This work was supported through both an NSF grant (EAR-0208312 to KXW) and an NSF Graduate Research Fellowship (to B.T.C.).

References

Berlin, M. M., and R. S. Anderson (2007), Modeling of knickpoint retreat on the Roan Plateau, western Colorado, *J. Geophys. Res.*, *112*, F03S06, doi:10.1029/2006JF000553.

Berryman, K., M. Marden, D. Eden, C. Mazengarb, Y. Ota, and I. Moriya (2000), Tectonic and paleoclimatic significance of Quaternary river terraces of the Waipaoa River, east coast, North Island, New Zealand, *N. Z. J. Geol. Geophys.*, *43*, 229–245.

Bigi, A., L. E. Hasbargen, A. Montanari, and C. Paola (2006), Knickpoints and hillslope failures: Interactions in a steady-state experimental landscape, *Spec. Pap. Geol. Soc. Am.*, *398*, 295–307.

Bishop, P., T. B. Hoey, J. D. Jansen, and I. L. Artza (2005), Knickpoint recession rate and catchment area: The case of uplifted rivers in eastern Scotland, *Earth Surf. Processes Landforms*, *30*, 767–778.

Crosby, B. T., and K. X. Whipple (2006), Knickpoint initiation and distribution within fluvial networks: 236 waterfalls in the Waipaoa River, North Island, New Zealand, *Geomorphology*, *82*, 16–38, doi:10.1016/j.geomorph.2005.1008.1023.

Davis, W. M. (1932), Piedmont bench lands and primaerruempfe, *Geol. Soc. Am. Bull.*, *43*, 399–440.

Eden, D. N., A. S. Palmer, S. J. Cronin, M. Marden, and K. R. Berryman (2001), Dating the culmination of river aggradation at the end of the last glaciation using distal tephra compositions, eastern North Island, New Zealand, *Geomorphology*, *38*, 133–151.

Fernandez Luque, R., and R. van Beek (1976), Erosion and transport of bedload sediment, *J. Hydraul. Res.*, *14*, 127–144.

Frankel, K. L., F. J. Pazzaglia, and J. D. Vaughn (2007), Knickpoint evolution in a vertically bedded substrate, upstream-dipping terraces, and Atlantic slope bedrock channels, *Geol. Soc. Am. Bull.*, *119*, 476–486, doi:10.1130/B25965.25961.

Gardner, T. W. (1983), Experimental study of knickpoint and longitudinal profile evolution in cohesive, homogeneous material, *Geol. Soc. Am. Bull.*, *94*, 664–672.

Gasparini, N. M., R. L. Bras, and K. X. Whipple (2006), Numerical modeling of non-steady-state river profile evolution using a sediment-flux-dependent incision model, in *Tectonics, Climate and Landscape Evolution*, edited by S. D. Willett et al., *Spec. Pap. Geol. Soc. Am.*, *398*, 127–141.

Gasparini, N. M., K. X. Whipple, and R. L. Bras (2007), Predictions of steady state and transient landscape morphology using sediment-flux-dependent river incision models, *J. Geophys. Res.*, *112*, F03S09, doi:10.1029/2006JF000567.

Gilbert, G. K. (1896), Niagara Falls and their history, in *The Physiography of the United States*, *Natl. Geogr. Soc. Monogr.*, vol. 1, edited by J. W. Powell, pp. 203–236, Am. Book, New York.

Haviv, I., Y. Enzel, K. X. Whipple, E. Zilberman, J. Stone, A. Matmon, and L. K. Fifield (2006), Amplified erosion above waterfalls and oversteepened bedrock reaches, *J. Geophys. Res.*, *111*, F04004, doi:10.1029/2006JF000461.

Hayakawa, Y., and Y. Matsukura (2003), Recession rates of waterfalls in Boso Peninsula, Japan, and a predictive equation, *Earth Surf. Processes Landforms*, *28*, 675–684.

Howard, A. D. (1980), Thresholds in river regimes, in *Thresholds in Geomorphology*, edited by D. R. Coates and J. D. Vitek, pp. 227–258, Allen and Unwin, Boston, Mass.

Howard, A. D. (1994), A detachment-limited model of drainage basin evolution, *Water Resour. Res.*, *30*, 2261–2285.

Howard, A. D., and G. Kerby (1983), Channel changes in badlands, *Geol. Soc. Am. Bull.*, *94*, 739–752.

Laity, J. E., and M. C. Malin (1985), Sapping processes and the development of theater-headed valley networks on the Colorado Plateau, *Geol. Soc. Am. Bull.*, *96*, 203–217.

Meyer-Peter, E., and R. Mueller (1948), Formulas for bed-load transport, paper presented at Second Congress, Int. Assoc. for Hydraul. Struct. Res., Stockholm, Sweden.

Montgomery, D. R. (2000), Coevolution of the Pacific salmon and Pacific Rim topography, *Geology*, *28*, 1107–1110.

Niemann, J. D., N. M. Gasparini, G. E. Tucker, and R. L. Bras (2001), A quantitative evaluation of Playfair's law and its use in testing long-term stream erosion models, *Earth Surf. Processes Landforms*, *26*, 1317–1332.

Paola, C., P. L. Heller, and C. L. Angevine (1992a), The large-scale dynamics of grain-size variation in alluvial basins, 1: Theory, *Basin Res.*, *4*, 73–90.

Paola, C., G. Parker, R. Seal, S. K. Sinha, J. B. Southard, and P. R. Wilcock (1992b), Downstream fining by selective deposition in a laboratory flume, *Science*, *258*, 1757–1760.

Parker, G. (2004), Somewhat less random notes on bedrock incision, *Int. Memo. 118*, 20 pp., St. Anthony Falls Lab., Univ. of Minn., Minneapolis.

Penck, W. (1924), *Die Morphologische Analyse: Ein Kapital der Physikalischen Geologie*, 200 pp., J. Engelhorns Nachf, Stuttgart, Germany.

Rosenbloom, N. A., and R. S. Anderson (1994), Hillslope and channel evolution in a marine terraced landscape, Santa Cruz, California, *J. Geophys. Res.*, *99*, 14,013–14,029.

Sklar, L. S., and W. E. Dietrich (1998), River longitudinal profiles and bedrock incision models: Stream power and the influence of sediment supply, in *Rivers Over Rock: Fluvial Processes in Bedrock Channels*, *Geophys. Monogr. Ser.*, vol. 107, edited by K. J. Tinkler and E. E. Wohl, pp. 237–260, AGU, Washington, D. C.

Sklar, L. S., and W. E. Dietrich (2004), A mechanistic model for river incision into bedrock by saltating bed load, *Water Resour. Res.*, *40*, W06301, doi:10.1029/2003WR002496.

Sklar, L. S., and W. E. Dietrich (2006), The role of sediment in controlling steady-state bedrock channel slope: Implications of the saltation-abrasion incision model, *Geomorphology*, *82*, 58–83, doi:10.1016/j.geomorph.2005.1008.1019.

Sklar, L. S., J. D. Stock, J. J. Roering, J. W. Kirchner, W. E. Dietrich, W. C. Chi, L. Hsu, M. L. Hsieh, S. J. Tsao, and M. M. Chen (2005), Evolution of fault scarp knickpoints following 1999 Chi-Chi earthquake in west-central Taiwan, *Eos Trans. AGU*, *86*(52), Fall Meet. Suppl., Abstract H34A-06.

Snyder, N. P., K. X. Whipple, G. E. Tucker, and D. J. Merritts (1999), Evidence for an equilibrium between main-trunk channel incision and tectonic uplift: Mendocino triple junction region, northern California, *Geol. Soc. Am. Abstr. Programs*, *31*, 444–445.

Snyder, N. P., K. X. Whipple, G. E. Tucker, and D. J. Merritts (2002), Interactions between onshore bedrock-channel incision and nearshore wave-base erosion forced by eustasy and tectonics, *Basin Res.*, *14*, 105–127.

Stock, J. D., and D. R. Montgomery (1999), Geologic constraints on bedrock river incision using the stream power law, *J. Geophys. Res.*, *104*, 4983–4993.

Tucker, G. E., and R. L. Bras (1998), Hillslope processes, drainage density, and landscape morphology, *Water Resour. Res.*, *34*, 2751–2764.

Tucker, G. E., and R. Slingerland (1996), Predicting sediment flux from fold and thrust belts, *Basin Res.*, *8*, 329–349.

Tucker, G. E., and R. L. Slingerland (1997), Drainage basin response to climate change, *Water Resour. Res.*, *33*, 2031–2047.

Tucker, G. E., and K. X. Whipple (2002), Topographic outcomes predicted by stream erosion models: Sensitivity analysis and intermodel comparison, *J. Geophys. Res.*, *107*(B9), 2179, doi:10.1029/2001JB000162.

Tucker, G. E., S. T. Lancaster, N. M. Gasparini, and R. L. Bras (2001a), The Channel-Hillslope Integrated Landscape Development model (CHILD), in *Landscape Erosion and Evolution Modeling*, edited by R. S. Harmon and W. W. I. Doe, pp. 349–388, Kluwer Acad., New York.

Tucker, G. E., S. T. Lancaster, N. M. Gasparini, R. L. Bras, and S. M. Rybarczyk (2001b), An object-oriented framework for distributed hydrologic and geomorphic modeling using triangulated irregular networks, *Comput. Geosci.*, *27*, 959–973.

van der Beek, P., and P. Bishop (2003), Cenozoic river profile development in the Upper Lachlan catchment (SE Australia) as a test of quantitative fluvial incision models, *J. Geophys. Res.*, *108*(B6), 2309, doi:10.1029/2002JB002125.

von Engeln, O. D. (1940), A particular case of knickpunkte, *Ann. Assoc. Am. Geogr.*, *30*, 268–271.

Waldbauer, H. (1923), Hängetäler im Oberengadin und Bergell, *Ostalp. Formenstud.*, *2*, 127.

Weissel, J. K., and M. A. Seidl (1997), Influence of rock strength properties on escarpment retreat across passive continental margins, *Geology*, *25*, 631–634.

Weissel, J. K., and M. A. Seidl (1998), Inland propagation of erosional escarpments and river profile evolution across the southeast Australian passive continental margin, in *Rivers Over Rock: Fluvial Processes in Bedrock Channels*, *Geophys. Monogr. Ser.*, vol. 107, edited by K. J. Tinkler and E. E. Wohl, pp. 189–206, AGU, Washington, D. C.

Whipple, K. X., and G. E. Tucker (1999), Dynamics of the stream-power river incision model: Implications for height limits of mountain ranges, landscape response timescales, and research needs, *J. Geophys. Res.*, *104*, 17,661–17,674.

Whipple, K. X., and G. E. Tucker (2002), Implications of sediment-flux-dependent river incision models for landscape evolution, *J. Geophys. Res.*, *107*(B2), 2039, doi:10.1029/2000JB000044.

Whipple, K. X., N. P. Snyder, and K. Dollenmayer (2000), Rates and processes of bedrock incision by the upper Ukak River since the 1912 Novarupta ash flow in the Valley of Ten Thousand Smokes, Alaska, *Geology*, *28*, 835–838.

Willgoose, G., R. L. Bras, and I. Rodriguez-Iturbe (1991), A coupled channel network growth and hillslope evolution model: 1. Theory, *Water Resour. Res.*, *27*, 1671–1684.

Wilson, K. C. (1966), Bedload transport at high shear stresses, *J. Hydraul. Eng.*, *92*, 49–59.

Wobus, C. W., B. T. Crosby, and K. X. Whipple (2006), Hanging valleys in fluvial systems: Controls on occurrence and implications for landscape evolution, *J. Geophys. Res.*, *111*, F02017, doi:10.1029/2005JF000406.

B. T. Crosby, Department of Geosciences, Idaho State University, Pocatello, ID 83209, USA. (crosby@alum.mit.edu)

N. M. Gasparini, Department of Geology and Geophysics, Yale University, New Haven, CT 06511, USA.

K. X. Whipple, School of Earth and Space Exploration, Arizona State University, Tempe, AZ 85287, USA.

C. W. Wobus, Cooperative Institute for Research in Environmental Sciences, University of Colorado, Boulder, CO 80309, USA.